Modelling hydrological and chemical phenomena during interaction of bentonite and high pH plume

Merja Tanhua-Tyrkkö
VTT

Pro Gradu
The University of Jyväskylä,
Physics department,
June 2009

ABSTRACT

In Finland the spent nuclear fuel is planned to be disposed of deep (~ 500m) in the crystalline Finnish bedrock. This repository concept is called KBS-3, where one of the important components is bentonite clay. One concern about bentonite is to assure its initially good features even in extreme conditions, like in the presence of high pH. The aim of this work is to learn how to model the interactions between the high pH plume and bentonite by using the TOUGHREACT code as a modeling tool.

The modeling is based on one experimental study, done in the framework of ECOCLAYII project within European Union's programme. The experiment consisted of small cylinder (length 12 cm and radius 2.5 cm) which was divided into two parts along the colon. The other half consisted of compacted bentonite clay and the other half was crushed rock powder. The high pH (12.5) plume was injected into the column from the bottom of the cylinder and the outflow water was collected from the other end. The experiment included transport and chemical phenomena, and thus, the code in TOUGHREACT was used. The main phenomena studied are cation exchange, pH evolution of the colon and mineral transformation of the bentonite.

In the modeling, the crushed rock is assumed to be inert, that is, it does not include chemical components. The bentonite consists of few minerals, of which montmorillonite causes the most important beneficial properties (like high cation exchange capacity, CEC) of bentonite. The cation exchange is modeled with the Gaines-Thomas convention, and the transport phenomena are advection in the crushed rock half and diffusion in the bentonite half. Furthermore, because the lack of TOUGHREACT's ability: to let CEC evolve during the modeling time, the montmorillonite is assumed not to dissolve.

As a result, the modelled cation exchange results agreed quite well to experimental results, whereas the pH results did not. In the experiment the bentonite seemed to buffer the highly alkaline pH whereas in the model it did not. This is probably because the rock was assumed to be inert and the montmorillonite did not dissolve. In addition, if the TOUGHREACT had an option to handle surface complexes, the pH buffering would be more reliable.

TIIVISTELMÄ

Suomessa käytetty korkea-aktiivinen ydinjäte on suunniteltu sijoitettavaksi syvälle (~500 m) Suomen kiteiseen kallioperään. Tämä loppusijoitussuunnitelma perustuu alun perin Ruotsissa kehitettyyn KBS-3 suunnitelmaan. Yksi tärkeä osa tätä suunnitelmaa on bentoniitti savi, joka sijoitetaan puskuri materiaaliksi kallion ja ydinjätteen väliin. Bentoniitti on valittu sen, loppusijoituksen turvallisuuden kannalta, hyvien ominaisuuksien vuoksi. Tällaisia hyviä ominaisuuksia ovat muun muassa bentoniitin suuri kationin vaihto kapasiteetti sekä bentoniitin paisumiskyky. Nämä bentoniitin hyvät ominaisuudet täytyisi pystyä säilyttämään äärimmäisissäkin olosuhteissa, kuten silloin jos pohjaveden pH jostain syystä nousee korkeaksi.

Tämän työn tarkoituksena on mallintaa (ja opetella mallintamaan) vuorovaikutusta korkean pH:n ja bentoniitin välillä, käyttäen TOUGHREACT koodia.

Mallinnus perustuu kokeelliseen ECOCLAY II tutkimukseen, joka tehtiin EU:n viidennessä puiteohjelmassa. Koe koostui pienestä sylinteristä joka oli 12 cm pitkä ja säteeltään 2,5 cm. Pitkittäissuunnassa sylinteri oli jaettu kahteen osaan, joista toinen puoli täytettiin kompaktoidulla bentoniitilla ja toinen puoli kivimurskeella (kivimurskeen rakojen koko ~1,5mm). Näin pakattuun sylinteriin syötettiin pohjasta korkean pH:n (12.5) vettä ja toisesta päästä vettä kerättiin analysoitavaksi.

Mallinnuksessa mielenkiinto oli kationin vaihto ilmiöissä, pH:n muutokset kolonnissa sekä bentoniitin mineraali muutokset.

Mallissa kivimurske oletettiin reagoimattomaksi. Sen sijaan bentoniitti oletettiin koostuvaksi eri mineraaleista, kuten montmorilloniitista, kipsisä ja albiitista. Näistä mineraaleista montomorilloniitti on kuitenkin se josta johtuvat bentoniitin yllä mainitut hyvät ominaisuudet. Kationin vaihtoa on kuvattu Gaines-Thomas-konventiolla. Kuljetusilmiöinä mallissa ovat: advektio (kivimurskeessa) ja diffuusio (kompaktoidussa bentoniitissa)

Lisäksi, koska TOUGHREACT koodissa ei ole mahdollisuutta antaa kationinvaihtokapasiteetin (CEC) muuttua mallinnuksen kuluessa, on montmorilloniitti oletettu liukenemattomaksi aineeksi.

Työn tuloksena huomattiin että mallin kationinvaihto tulokset vastasivat hyvin kokeellisia arvoja, kun taas pH ei puskuroitunut mallissa lainkaan, vaikka kokeellisessa työssä näin oli käynyt. Korkea pH mallissa johtuu todennäköisesti seuraavista syistä: kivimurske oletettiin reagoimattomaksi sekä siitä että montmorilloniitti ei liukene. Lisäksi jos TOUGHREACT koodissa olisi mahdollisuus käsitellä pintakomplekseja, saattaisi pH:n puskurointikyky olla todenmukaisempi.

Kokeellisessa aineistossa mineraalien muuntumista ei juurikaan ollut tutkittu, joten vertailua kokeellisen työn ja mallin välillä ei juurikaan voida tehdä. Kokeellisessa työssä kuitenkin huomattiin että kolonnin pinnalle oli muodostunut geelimäistä ainetta, joten oletuksen uusien faasien muodostumisesta voi tehdä. Mallinnuksen tuloksena syntyi myös muutamia uusia faaseja mutta niiden osuus kokonaistilavuusosuudesta oli

lähes olematon. Syy pieniin tilavuusosuuksien muutoksiin johtunee valinnoista joissa huokoisuus pysyy vakiona, sekä oletuksesta montmorilloniitin liukenemattomuudesta.

TABLE OF CONTENTS

LIST OF SYMBOLS USED

A	surface area [g/cm^2] of mineral m
C	water's conductivity [m/s]
CEC	cation exchange capacity [eq/kg]
CSH	calcium-silicate-hydrate
D_w	diffusion coefficient of water
F^κ	mass (or heat flux) [kg/m^{2}s]
g	gravity
K	equilibrium coefficient
k	permeability
l_c	length of curve
I	ionic strength
IAP	ion activity product (sometimes marked with Q)
M^κ	mass accumulation term [kg/m^3]
m	
n	normal vector on surface Γ_n
p	pressure
Q	ion activity product (sometimes noted also as IAP)
q	sink or source
S_β	saturation of phase β
SI	saturation index
t	time (usually in seconds)
u	the seepage velocity or Darcy's velocity
V	volume
V_n	volume of grid block n [m^3]
X^κ_β	mass fraction of phase β
x	distance
z	ion's charge
$å$	coefficient in Debye-Hückel equation

Greek letters

α	coefficient in Debye-Hückel equation
Γ	surface
γ	activity coefficient
κ	the of components in flow system
μ	viscosity
ρ	density
τ	tortuosity
υ	kinematic viscosity
φ	porosity
Ω	mineral saturation ratio
ω	coefficient in Debye-Hückel equation

Brackets	
$[B^z]$	ion B with charge z in **square brackets** denotes the **concentration** of ion B
$\{B^z\}$	ion B with charge z in **curled brackets** denotes the **activity** of ion X

FOREWORD

This work was done at VTT (Technical Research Centre of Finland) in co-ordination with Posiva Oy. The work was mainly tutored by Markus Olin and the supervisor from the University of Jyväskylä was Markku Kataja.

Great commendations go also to Jarmo Lehikoinen (B+Tech Oy) whose has endless interest to modelling these phenomena. In addition his sense of humour for my frustration is sui generis.

I would also thank my workmates, specially Riitta and Arvo; no one else can make such a delicious borsch!

Thanks belong also to my nearest relatives and friends: lots of love for those who understand how much they mean to me, and lost of anger for those who make that look ridiculous.

Otaniemi, Espoo 27.6.2009
Merja Tanhua-Tyrkkö

1 INTRODUCTION

The nuclear power is an effective way to produce energy. Unfortunately the use of nuclear power causes a problem of spent fuel, which is highly radioactive, which radioactivity will last hundreds of thousands of years and thus it is a problem, not only for people today but also, for new generations.

All in all the nuclear power plants produce nowdays 60 tons of spent fuel per year in Finland. For the meantime the used fuel has been stored in large water tanks at nuclear power plants, but these tanks are not considered as the solution for final disposal. Thus there are plans for more secure systems.

Nowadays there are mainly two ways to handle this waste: either to return it to fuel cycle or use it only once **[STUK, 2008]**. Anyhow neither of these handling processes do not significantly reduce the amount of nuclear waste or, unfortunately, the longlasting radioactivity. Thus the nuclear waste needs to be disposed in a place where it is in safe and will not jeopardize the biosphere. For this reason many nuclear power-producing countries, including Finland, have planned[1], a geological repository for the nuclear waste. These repositories consist of many natural and engineering barriers, which are designed to prevent or at least retard the movement of radioactive nuclides into biosphere.

The Finnish plan for this preventing and retarding barrier system follows the Swedish design, so called KBS3-V concept, see **Figure 1**.

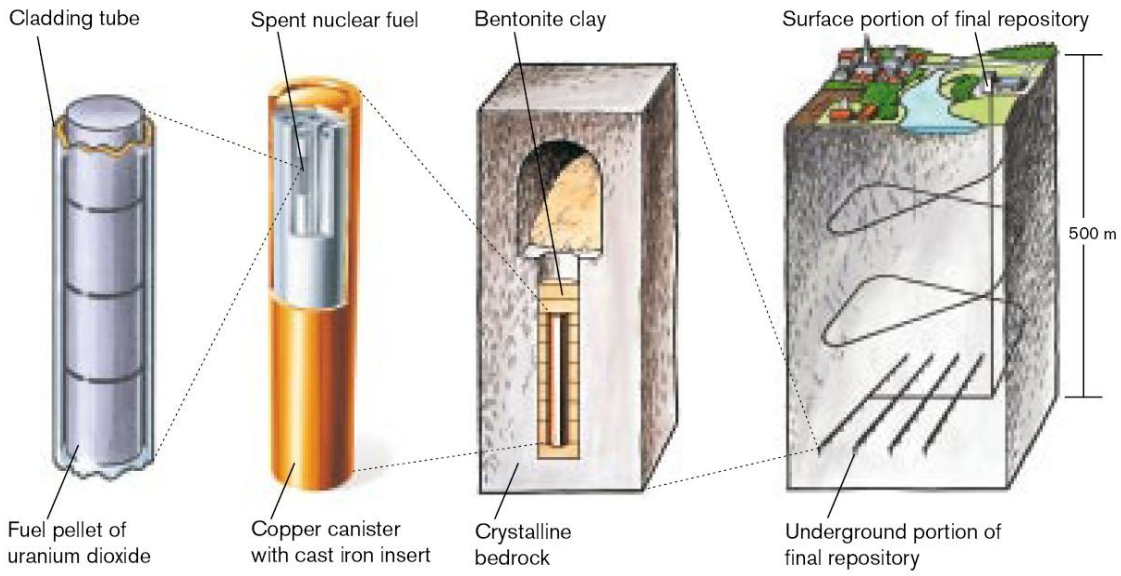

Figure 1. The planned disposal concept for high-level nuclear waste **[SKB, 2006]**.

[1] Note! planned not implemented

The design consists of copper canister, bentonite clay and host rock, also some cementitious materials are used to seal the repository. The waste is going to be encapsulated in iron-contained copper-canisters and buried 500 m deep in host rock. Bentonite clay is used as buffer between the rock and canister.

Thus the repository consists of various natural and engineering barriers which first of all isolate the waste from biosphere and second of all, if some barrier is impaired, the other barriers will retard the movement of the radionuclei.

In case if the canister shatters, the bentonite clay has an important role in retarding the transport of radionuclei because, according to the design, in wet bentonite the radionuclei will transport slowly by diffusion. Another function of bentonite is its great cation exchange capacity. More profound description of the repository and functions of repository's barriers, including bentonite, can be found from **[Pastina & Hellä, 2008]**.

In this work the interest is on interaction between the bentonite clay and high pH plume. The significance of the interaction between bentonite and alkaline water is quite relevant because there will be cementitious materials used in the repository and these materials are known to have high pH. Thus the question will be: does the high pH plume damage the bentonite; will it transform the minerals of bentonite so that the composition or performance of bentonite changes?

That is the question asked, but not fully answered. There are few experiments done, concerning interactions between bentonite and alkaline water, but all of these have at least one problem: the short duration. The experiments have lasted only few years and this rises up a problem, what will happen if the high pH plume is in contact with bentonite longer time, like hundreds of thousands of years which is the case in deep repository. Anyhow an experiment lasting that long is quite unrealistic and thus the computing capability of computers is harnessed to solve (or at least try to solve) these problems. There is also need for those who harness the computers, thus this work is done.

In this work the main target is to learn how to model the interaction between bentonite and high pH plume and learn more about the phenomena involving this interaction. This work is also part of VTT's aim to train new people to model coupled problems between hydrological and chemical phenomena and furthermore, in future, couple these phenomena to thermal and mechanical processes, which are assumed to happen in the spent fuel repository.

For this modelling-training process, one experimental work, done by **[Vuorinen et al., 2006]**, was chosen to be modelled. The experimental set-up can be found from **chapter 2** and needed parameters from **chapter 1** and parameter values are also collected in **Appendix A**.

At the beginning of this work there were few proposals for the modelling tool. The candidates were EQ3/6 **[Wolery & Jarek, 2003]**, COMSOL Multiphysics **[The**

COMSOL Group, 2009] and PetraSim **[Thunderhead engineering, 2005]**. The EQ3/6 is good modelling tool when concerning the chemical reactions but it lacks transport phenomena (diffusion and Darcy's flow) and COMSOL Multiphysics is good tool when transport phenomena are modelled but the chemical modelling seems clumsy compared to EQ3/6 (and PetraSim). From these three options the PetraSim was chosen because it couples the thigs which the previous tools lack: the transport and chemical phenomena.

Hence the modelling tool is PetraSim which is the graphical interface for the TOUGH family of codes. From the TOUGH family of codes the TOUGH2 and TOUGHREACT was the one used. More of these codes are presented in **chapter 3**.

When modelling the experimental work the first note is that it is very rare that the modelling code and the experiment correspond fully o each other, thus there must be some pre-calculations before the parameters from experiment can be fed to the model. More about these parameters is described in **chapter 4** and **Appendix A**. The results from the modelling part are written in **chapter 5** and discussed in **chapter 6**. Finally the work is concluded in **chapter 7**.

2 THE EXPERIMENT MODELLED

The experiment, which is modelled, was done in the framework of the ECOCLAY II project **[Huertas et al., 2000]**. The experiment's purpose was to study processes occurring in interaction between bentonite and high pH plume like: diffusion, cation exchange and (little bit) mineral alterations. Also mineral alterations in crushed rock were under interest. The experiment **[Vuorinen et al., 2006]** consisted of two different experiments: the batch experiment and flow-through experiment. For the "learn to model"-purposes the flow-through one was selected and therefore only it is discussed here.

The used experimental set-up for flow-through experiment is illustrated in **Figure 2**. The set-up consisted of closed cylinder[2] which was filled with bentonite and crushed rock powder. Half of the cylinder was bentonite and other half was crushed rock. The cylinders were placed vertically (in other words, turn the **Figure 2** 90° to the left).

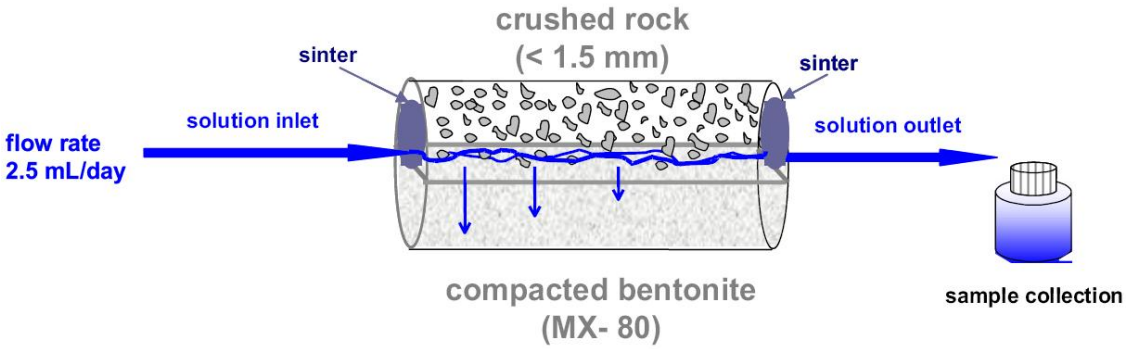

Figure 2. Schematic view of the experimental set-up used in the flow-through experiment, from **[Vuorinen et al., 2006]**. In reality the cylinder was placed vertically (meaning that turn the figure 90º to the left, resulting the inlet end is at the bottom and the outlet end at top)

In flow-through experiment there were three waters with different compositions; fresh water (ALL-MR), saline water (OL-SS) and saline-alkaline (OL-SA). Anyhow, in this *modelling work* only the OL-SA water, was under interest and thus only its composition is presented in **Table 1**. This selection was made because of the most alterations in bentonite were considered to occur in the presence of alkaline plume.

[2] The cylinder was 11.6 cm long with diameter of 5cm.

Table 1. The composition of the in-flow water.

	OL-SA [mol/L]
pH	12.5
H^+	$5.985*10^{-13}$ [3]
Na^+	0.428
Ca^{2+}	0.018
Cl^-	0.462
Ionic strength	0.46
Al^{3+}	$1.0*10^{-20}$
Other species (K^+, Mg^{2+}, $H_4SiO_4(aq)$, SO_4^{2-})	1.0e-8

The water was injected from bottom and water samples were collected at top **Figure 2**. In the experiment both the solution inlet and outlet was assembled in the crushed rock part thus the interaction, between crushed rock and bentonite, was allowed only by diffusion.

For the experiment there were two similar cylinders, described above, for two different time periods: 1 year (360 days, $31.1 \cdot 10^6$s) and 1.5 years (560 days, $48.4 \cdot 10^6$s).

After the experiment the cylinder were sectioned into smaller parts according to **Figure 3.** To clarify the analyses the sections were coded with letters: A, B, … , F.

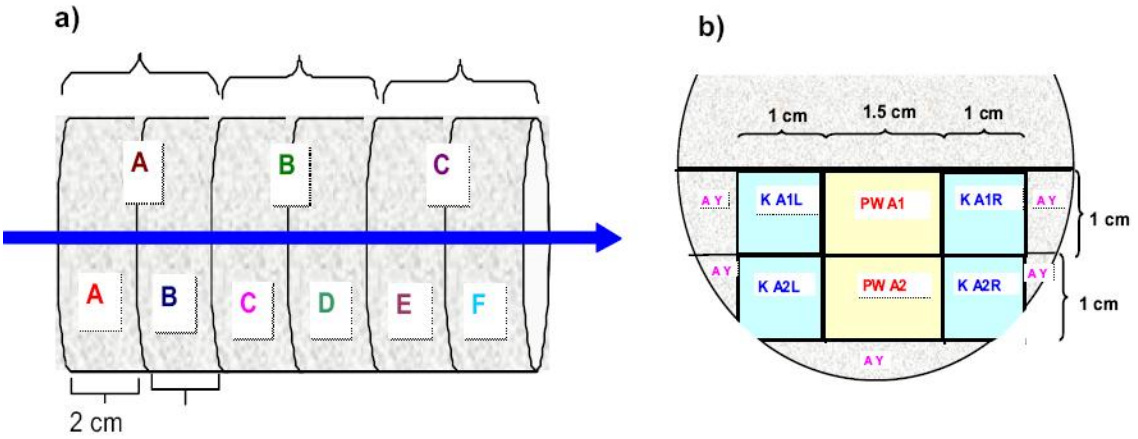

Figure 3. Sectioning of the flow-through cylinders.

[3] Note that here the ionic strength has been taken into account thus pH=-log{H^+}, see more about the symbols from chapters later on.

3 THE THEORY BEHIND THE MODELLING PROCEDURE

Even though the experimental system (described in previous chapter) seems quite simple system; in modeller's eyes it is a bunch of difficult phenomena. It consists of mass transfer (diffusion) and momentum transfer (Darcy's law), chemical equilibrium, mineral equilibrium, cation exchange, surface complexes and, worst of all, these all may interact with each other. Therefore if this kind of system is wanted to be modelled, there is a need for various mathematical equations and in addition because all the phenomena interact with each other, the equations need to be coupled with each other.

This coupling is implemented in few programs like PHREEQC**[Parkhurst & Appelo, 1999]**, Geochemist Workbench **[Bethke & Yeakel, 2009]**, etc. In this work the modelling program used was anyhow PetraSim which is a graphical interface for TOUGH code-family: TOUGH2, T2VOC, TMVOC, TOUGHREACT and TOUGH-Fx/HYDRATE. In this work the main emphasis is on TOUGHREACT and TOUGH2.

With TOUGH2 you can model problems which include non-isothermal flow of multi-component[4], multiphase[5] fluids in one-, two- or three-dimensional porous and fractured media and TOUGHREACT is a code which **adds chemical reactions** to that flow. To understand the code's calculating procedure, the following equations need to be understood.

3.1 Mass and energy balance

The mass balance for solute c can be described with a help of **Figure 4**

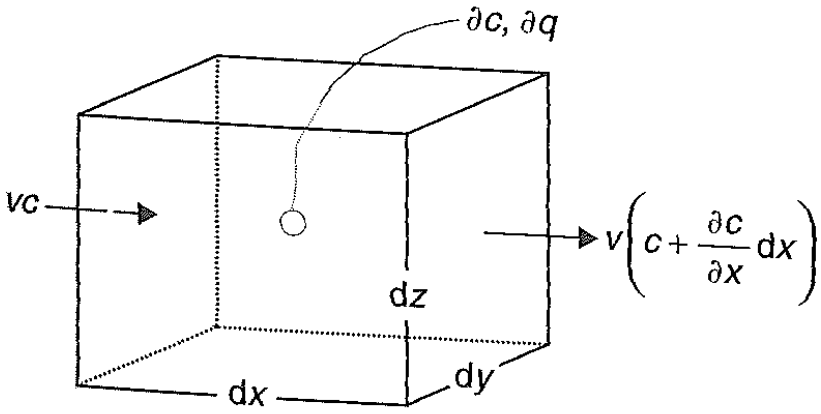

Figure 4. Mass balance of solute transport through a cube, from **[Appelo & Postma, 2005]**

The solute enters the cube in x-direction with a velocity v and thus the mass balance for the solute is described as

[4] In this component means mainly water or air.
[5] And phase means liquid or gas.

rate of accumulation in control volume
= rate of input to control volume - rate of output from control volume (3-1)
- rate of sorption in control volume

To get the rate of accumulation over the whole studied area, all control volumes need to be summed up, i.e. integrated over the total volume.

Thus in mathematical form:

$$\frac{d}{dt}\int_{V_n} M^{\kappa} dV_n = \int_{\Gamma_n} \bar{F}^{\kappa} \cdot \bar{n}\, d\Gamma_n + \int_{V_n} q^{\kappa} dV_n \qquad (3\text{-}2)$$

that is the equation which TOUGH2 solves.

So the equation denotes that the integration is over volume V_n which is bounded by closed surface Γ_n. The accumulation term M represents the mass or energy per volume. The label κ, above the accumulation term M, denotes the mass components (and the heat "component" if the calculated system is nonisothermal). Furthermore the vector **F** represents the mass or heat flux, vector **n** is the normal vector on surface element $d\Gamma_n$, which points inward to V_n and q denotes the source or sink. More details of **equation (3-2)** can be found from **[Xu et al., 2004]**.

3.2 Transport phenomena

For flow in porous media the main concepts are flow in porous medium which is described by Darcy's law, relative permeability capillary pressure and diffusion.

In PetraSim there are few options to calculate the permeability changes in material. These options assume that the relative permeability is dependent on porosity variation. In this work, though, it was decided that the porosity will stay constant during the calculation. Thus the relative permeability is not discussed here.

Neither the capillary pressure were not taken into account in this model, further information about the relative permeability and capillary pressure equations the reader is referred to TOUGH2 manual **[Pruess et al., 1999]** and TOUGHREACT manual **[Xu et al., 2004]**.

3.2.1 Darcy's law

Behind all the TOUGH-family codes there is an assumption that flow follows Darcy's law. Darcy's law assumes that the instantaneous charge (Q, [m^3/s]) is directly proportional to the hydraulic gradient ((h_1-h_2)/l) between two points (1 and 2) see **Figure 5**.

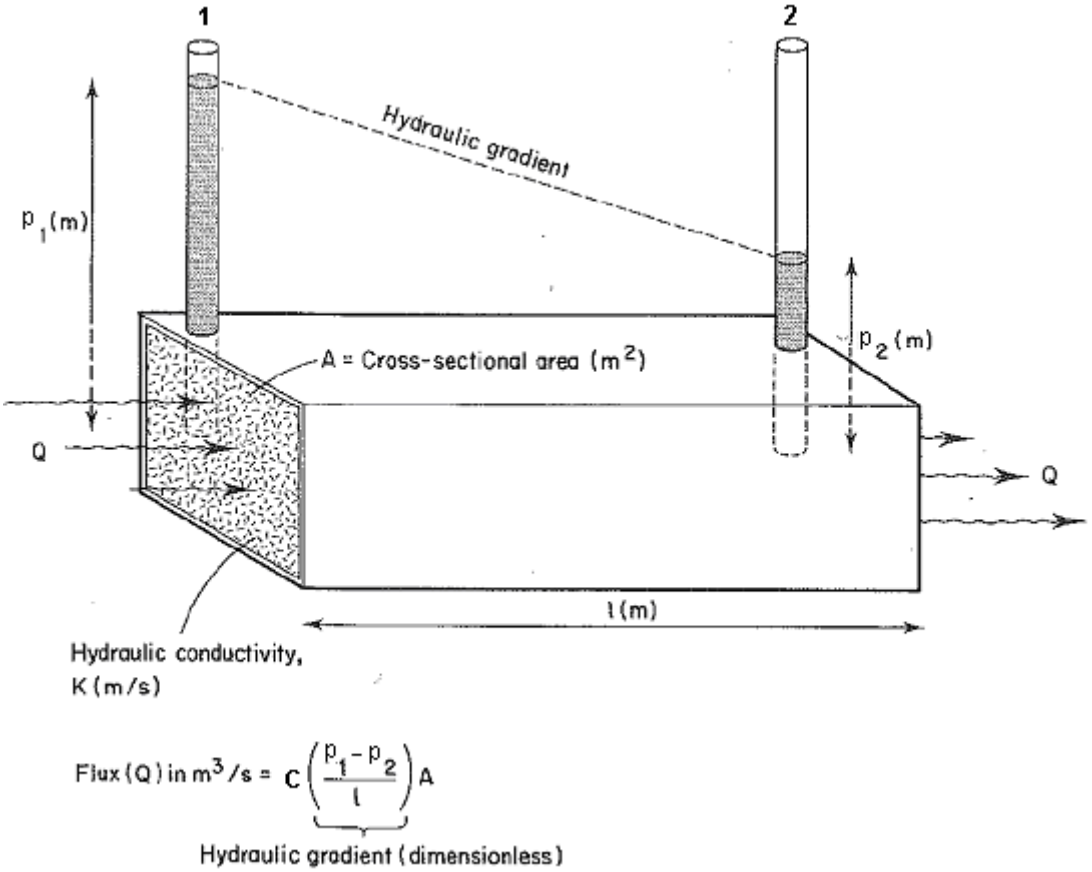

Figure 5. The schematic presentation of Darcy's law. Modified from **[Chapman & McKinley , 1987]**.

In mathematical form of the Darcy's law for single phase, is presented in **equation (3-3)**

$$Q = -C\frac{\Delta p}{l}A \tag{3-3}$$

where C is hydraulic conductivity [m/s], l is the distance between points 1 and 2 [m]. The minus sign denotes the fact that fluids flow naturally from high pressure to low pressure.

When the **equation (3-3)** is divided by cross-sectional area A [m^2] we get a equation for seepage velocity **u**:

$$\bar{u} = -C\left(\Delta p - \rho\bar{g}\right) = -\frac{k}{\mu}\left(\Delta p - \rho\bar{g}\right) \tag{3-4}$$

where the **u** is a seepage velocity vector (or Darcy's velocity), k is total permeability, μ is viscosity of water, p is the pressure, ρ is water density and g is acceleration due to gravity.

Darcy's law can also be extended to multiphase flow but in this work it is not necessary because the modelled experiment was executed in isothermal conditions (25°C). More about Darcy's law for multiphase flow can be found from TOUGH2 and PetraSim manuals **[Pruess et al., 1999]**, **[Thunderhead engineering, 2005]**.

3.2.2 Diffusion

The mass or solute transport between two points is not necessary driven by pressure drop but also by concentration differences.

A concentration difference, between two points in a solution, will be levelled out in time by the Brownian movement of molecules Figure 6. This process is called diffusion and is described by Fick's laws e.g. **[Appelo & Postma, 2005]**.

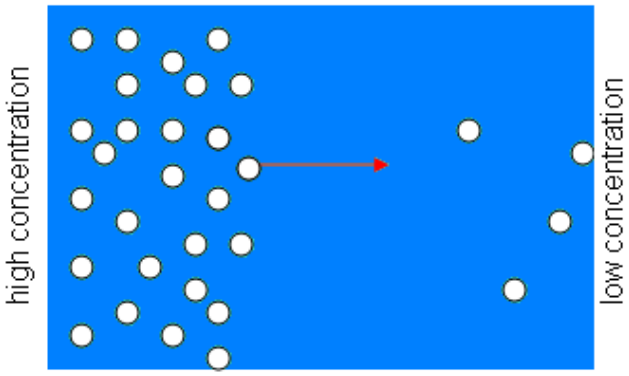

Figure 6. Schematic view of the diffusion of species (white circles) in free water.

The experimental results indicates that the diffusion flux f [1/m^{2}s] in free water follows the equation

$$f = -D_w \frac{\partial c}{\partial x} \tag{3-5}$$

where D_w is the diffusion coefficient for the species [m^2/s] and the c is the concentration of the species. The minus sign arises from the fact that species moves from high to low concentration thus the gradient $\partial c/\partial x$ is negative.

3.2.3 Other concepts related to transport phenomena

Porosity

The material's porosity φ is defined to be the ratio of the pores' volume in material V_{pores} to the total volume V_{total}, see **equation (3-6)**

$$\varphi = \frac{V_{pores}}{V_{total}} \tag{3-6}$$

In other words the porosity can be described as empty space divided by the total volume.

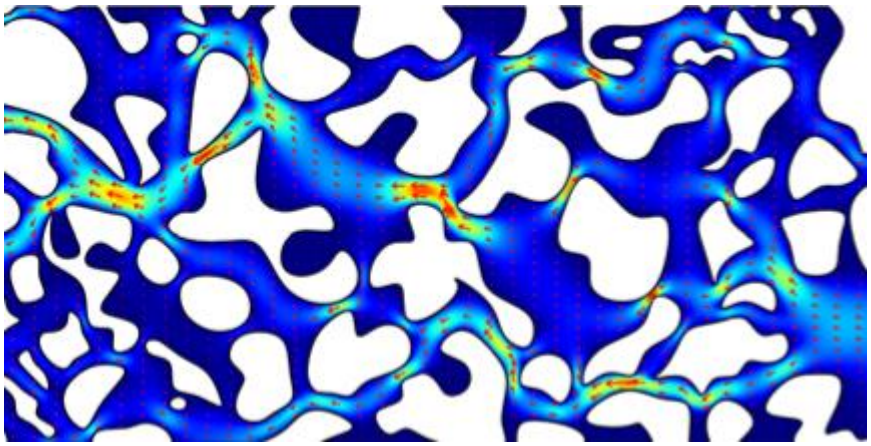

Figure 7. Schematic view of pores (the coloured areas) in mineral (white area). The figure is from COMSOL Multiphysics – Model Library **[COMSOL AB , 2008].**

Tortuosity
Tortuosity is a quantity which describes the twisted or winding nature of the porous material. It is an empirical factor thus described differently for different materials. In this work the tortuosity is described for bentonite and crushed rock, **chapter 4.6**.

3.3 Chemical phenomena

The experiment described above consists of many chemical reactions and thus many different models. The **Figure 8** illustrates the different chemical phenomena which one species (in this example the species is Ca^{2+}) may undergo.

First of all the species (Ca^{2+}, $CaOH^{+}$, other species) are in water environment. The species may react in water and form aqueous complexes ($Ca(OH)_2(aq)$) or precipitate on/in solid and form mineral ($Ca(OH)_2(s)$). The amount of the species in water may also increase as a result of dissolution of the solid, or decrease as a result of cation exchange. It is also known that the species may form surface complexes. In this work, though surface complexes are ignored because the used code (PetraSim) does not handle them.

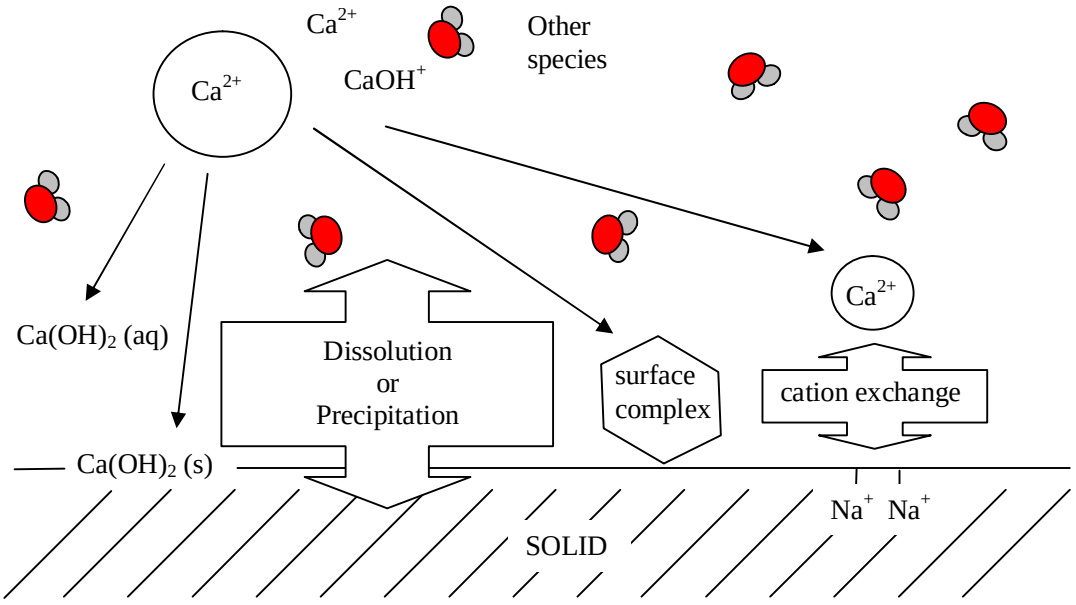

Figure 8. Examples of competing chemical reactions for Ca^{2+} in geochemical modelling.

To illustrate these phenomena, see **Figure 8**, there is a set of equations, which describe these phenomena in mathematical form. These equations are collected under the theory of chemical thermodynamics. In the next chapters the idea is go briefly through those parts and consepts of thermodynamics which are relevant *in this work*.

3.3.1 Chemical equilibrium

Chemical reactions in equilibrium can be written in a form:

$$aA + bB \Leftrightarrow cC + dD \qquad \text{Reaction 1.}$$

in which a moles of A reacts with b moles of B and from this reaction the result is c moles of C and d moles of D.

The species A and B are called the reactants and C and D the products. Furthermore, the coefficients a, b, c and d are called the stoichiometric coefficients. The arrow between the reactants and products indicates the "direction" of the reaction. The reaction can be proceeding to the right[6] or reach equilibrium. This proceeding is described with arrow to the right (or to the left) if all of the reactants are transforming to product species. Whereas the reaction is not proceeding to any direction the reaction (like in **reaction 1**) is indicated with double-ended arrow, in this case the reaction is considered to be in equilibrium.

[6] or why not to the left, but then the reactants and products in our example reaction (**reaction 1**) change places.

When the **Reaction 1** *is* in equilibrium it is described by equilibrium constant[7] *K* which is defined to be

$$K = \frac{[C]^c [D]^d}{[A]^a [B]^b} \tag{3-7}$$

where the squared brackets denotes the concentration of the species. **Equation (3-7)** is in fact called the law of mass action. More about the law of mass action can be found from **[Reichl, 1980]**.

If e.g. **Reaction 1** is not in equilibrium the product in **(3-7)** is called an ion activity product (IAP) or reaction quantity Q. The IAP is defined similarly to equilibrium constant but it should be noted that the concentrations in IAP's definition are not same as when the reaction is in equilibrium.

At this point to fully understand the differences between equilibrium constant and IAP the reader is preferred to get familiar with the mass action law and its connection to Gibbs energies from, for example, book **[Anderson, 2005]**.

Activity coefficients

Concentration values used in the equilibrium **equation (3-7)** above considers only situation where the species are in system with no other ions present. Thus the equation does not take into account how the ion behaves if there are other ions in the solution, for this reason the concept of activity and activity coefficient has been introduced.

In pure water the activity coefficient is unity but if salt concentration increases the aqueous species moves closer together and thus are more likely to come in contact **[Langmuir, 1997]**. Furthermore in solution where are other ions present also the Coulombic forces between the ions affects the behaviour of the ions.

Like, for example, a Ca^{2+} ion in solution, see **Figure 9**: the negative side of dipole water molecule surround positively charged calcium ion thus the water molecules, in a way, "shade" the behaviour of this cation. Thus, the reactions in solution need to be written in terms of activities instead of concentrations.

[7] NOTE that the equilibrium constant is also called the selectivity coefficient or exchange coefficient depending on source and in fact on reaction. The selectivity and exchange coefficient are usually used when writer is talking about the cation exchange.

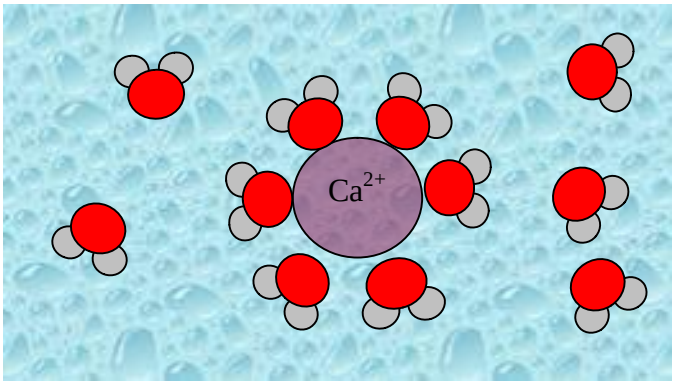

Figure 9. The water molecules surround the cation and thus "shields" cation's activity. (The figure is not in scale.)

Tough there is a need to define a quantity called activity {C}, which describes the activity of the species *C* though it is defined to be:

$$\{C\} = \gamma[C] \tag{3-8}$$

where squared brackets indicate the concentration of ion *C* and γ is the activity coefficient.

All in all the effects described above are included into the activity coefficient, which can be calculated by using theoretical Debye-Hückel-equation **(3-9)**.

$$\log \gamma_i = -\frac{\alpha z_i^2 \sqrt{I}}{1+\omega\sqrt{I}} \tag{3-9}$$

where α and ω are parameters derived by **[Helgeson & Kirkham, D. H. and Flowers G. C., 1981]** and I is ion strength defined in:

$$I = \frac{1}{2}\sum_i \left([X_i] z_i^2\right) \tag{3-10}$$

where squared brackets indicate ion's concentration and z is the charge of that ion.

Thus the activity coefficient of the species, indicates how effective the species is and furthermore the activity coefficient is dependent on the surrounding species and the effect of surrounding species is described by ionic strength.

The form of Debye-Hückel **equation (3-9)** varies with different ion strengths. More about these is told in e.g. **[Stumm & Morgan, 1996]**.

TOUGHREACT uses an extended version of **Debye-Hückel** equation, which is represented in TOUGHREACT manual, Appendix H **[Xu et al., 2004]**

3.3.2 Chemical equilibrium with activity

For the reasons explained above we modify the **equation (3-7)** to a form where the activities have been taken into account; thus the equilibrium constant need to be written:

$$K = \frac{\{C\}\{D\}}{\{A\}\{B\}} = \frac{\left(\gamma_c [C]\right)^c \left(\gamma_d [D]\right)^d}{\left(\gamma_a [A]\right)^a \left(\gamma_b [B]\right)^b} \tag{3-11}$$

where curved brackets {} denotes the activities and squared [] the concentrations. The original brackets () denotes just mathematical calculation order.

Equations for cation exchange and equivalent fraction

For cation exchange calculations the PetraSim has three different options. The cation exchange can be calculates by using Vanselow, Gaines-Thomas or Gapon conventions. In this work it has been decided to use the Gaines-Thomas convention and thus only it is presented here. For more information about the other conventions the reader is referred to **[Appelo & Postma, 2005]**.

The cation exchange in chemical form is:

$$\mathrm{NaX} + \frac{1}{2}\mathrm{Ca}^{2+} \Leftrightarrow \frac{1}{2}\mathrm{CaX_2} + \mathrm{Na}^{+} \qquad \text{Reaction 2}$$

where X^- represents one mole of the exchanger (in this work montmorillonite). This reaction has equilibrium constant $K_{Na/K}$ which is according to definition:

$$K_{Na/Ca} = \frac{\{\mathrm{NaX}\}\{\mathrm{Ca}^{2+}\}^{\frac{1}{2}}}{\{\mathrm{CaX_2}\}^{\frac{1}{2}}\{\mathrm{Na}^{+}\}} = \frac{\{\mathrm{NaX}\}\gamma_{Ca^+}^{\frac{1}{2}}\left[\mathrm{Ca}^{2+}\right]^{\frac{1}{2}}}{\{\mathrm{CaX_2}\}^{\frac{1}{2}}\gamma_{Na^+}\left[\mathrm{Na}^{+}\right]} \tag{3-12}$$

where curved brackets denotes the activity of the ion or the compound and squared brackets the concentrations. The activities of NaX and CaX_2 are approximated by their equivalent fractions β_{CaX} and $\beta_{NaX.}$

Equation (3-12)can be expressed with equivalent fractions:

$$K_{Na/Ca} = \frac{\beta_{\mathrm{NaX}}\gamma_{\mathrm{Ca}^+}^{\frac{1}{2}}\left[\mathrm{Ca}^{2+}\right]^{\frac{1}{2}}}{\beta_{\mathrm{CaX_2}}^{\frac{1}{2}}\gamma_{\mathrm{Na}^+}\left[\mathrm{Na}^{+}\right]} \tag{3-13}$$

3.3.3 Reaction kinetics: dissolution and precipitation

In the previous chapter it was assumed that the reactions reach the equilibrium instantly. Anyhow in most cases the reaction will not reach the equilibrium right a way, like most minerals which form in the course of time. In these cases there are few additional equations which need to be used.

The saturation index for minerals

First we define the saturation index for minerals because it is needed in following section.

The thermodynamic saturation state of mineral relative to the aqueous solution, Ω, is defined by

$$\Omega = \frac{IAP}{K} \tag{3-14}$$

where IAP is the ion activity product and K is equilibrium constant.

The saturation index indicates the saturation state of mineral in solution.

$$SI_m = \log_{10} \Omega_m \tag{3-15}$$

So when the saturation index SI is 0 the reaction is in equilibrium, whereas if the $SI > 0$ the solution is oversaturated with respect to the mineral in question and undersaturated if $SI < 0$.

> Note that when the reaction is in equilibrium, then the mineral saturation ratio is:
>
> $$\Omega = \frac{IAP}{K} = 1 \qquad \Leftrightarrow \qquad IAP = K$$
>
> As mentioned in chapter 3.3.1 note also that even though K and IAP have same form **equation 3-7** still K stands for activities at equilibrium where as IAP for activities in water sample **[Appelo & Postma, 2005]**.

Equilibrium/kinetic mineral dissolution/precipitation

In TOUGHREACT (and thus in PetraSim) for mineral dissolution/precipitation calculations the following rate expression is used:

$$r_m = f\left(c_1, c_2, ..., c_{N_C}\right) = k_m A_m \left|1 - \Omega_m^{\theta}\right|^{\eta} \qquad m = 1,...,N_q \qquad (3\text{-}16)$$

where positive results for r_m indicate dissolution and negative values precipitation. Other parameters k_m, A_m and Ω_m see **equation (3-14)**, indicates rate constant (moles per unit mineral surface area and unit time), specific reactive surface area per kg H_2O and mineral saturation ratio (**equation (3-16)**), respectively.

> Note also that when the mineral dissolution/precipitation reaction is in equilibrium the mineral saturation ratio Ω is one.

The rate constant k_m in **equation (3-16)** , as obvious, describes the "speed" of the reaction. This "speed" is generally known to be dependent on pH[8]. Thus PetraSim calculates the value of k_m by using **equation (3-17)**

$$k_m = k_T^{neutral} e^{\left[\frac{-E_a^{neutral}}{R}\left(\frac{1}{T}-\frac{1}{283.15}\right)\right]} + k_T^{H} a_H^{n_H} e^{\left[\frac{-E_a^{H}}{R}\left(\frac{1}{T}-\frac{1}{283.15}\right)\right]} + k_T^{OH} a_{OH}^{n_{OH}} e^{\left[\frac{-E_a^{IH}}{R}\left(\frac{1}{T}-\frac{1}{283.15}\right)\right]} \qquad (3\text{-}17)$$

where the k_T denotes the rate constant at temperature T (K) and superscript above indicates the pH range where the rate constant has been measured. furthermore the parameter a is the activity of the species (H^+ or OH^-) and n is a power term (constant). In **equation (3-17)** the acid area is considered to be when the pH is 0-4, neutral when the pH is 4-6 and base when pH is 8-14.

In addition the parameters in exponent are E, which is the activation energy, R is the gas constant and T is as mentioned temperature at kelvins. In this work the temperature is normal room temperature (25ºC), though the exponent is zero and thus the k_m follows the **equation (3-18)**.

$$k_m \overset{\text{in this work}}{=} k_{283.15}^{neutral} + k_{283.15}^{H} a_H^{n_H} + k_{283.15}^{OH} a_{OH}^{n_{OH}} \qquad (3\text{-}18)$$

The used parameters for equation (3-18) are listed in **Table 2**

[8] Of course these phenomena are also dependent on temperature (T) but in the experiment in question was examined in constant temperature in this case it needs not to be taken into account.

Table 2. The parameters for kinetic reactions. The parameters are collected from [Palandri & Kharaka , 2004] unless noted otherwise.

Mineral	***Dissolution and precipitation parameters***				
	Neutral mechanism	*Acid mechanism*		*Base mechanism*	
	k_{25} *[mol/m^2/s]*	k_{25}	$n(H^+)$	k_{25}	$n(H^+)$
Primary minerals:					
Albite	*0.28E-12*	*69.18E-12*	*0.317*	*0.25E-15*	*-0.471*
Cristobalite	*0.49E-12*				
Gypsum	*0.002*	*No additional mechanisms*			
Muscovite	*0.03E-12*	*1.41E-12*	*0.37*	*2.82E-15*	*-0.22*
Quartz	*0.01E-12*	*Not available*		*0.05E-15*	*-0.5*
Secondary minerals:					
Brucite	*5.75E-9*	*18.6E-6*	*0.5*	*Not available*	
Gibbsite	*3.16E-12*	*22.4E-9*	*0.992*	*0.02E-15*	*-0.784*
K-feldspar	*0.39E-12*	*87.1E-12*	*0.5*	*6.31E-12*	*-0.823*
Ettringite, Friedel_Salt, Hydrotalcite, Katoite, Monosulfoaluminate, Portlandite, Straentlingite, Tobermorite, Tobermorite_14A	*0.10E-9 (*)*	*No additional mechanisms*			
(Hydrogarnet, CSH_0.0(**), CSH_0.4, CSH_0.8, CSH_1.2, CSH_1.667)	*assumed at equilibrium*				

(*) this number was selected because it was noted that in some cases the used program crashed without this.
(**)CSH_x, where CSH is Calcium Silicate Hydrate, and x is the calcium-to-silica ratio.

3.3.4 Surface area

In **equation (3-16)** there were also a quantity A_m which is called as the specific surface area, with unit cm^2/g. The concept of surface area is used because the *whole amount* (volume fraction) of certain mineral, in material, *will not react* with the surroundings. It is assumed that most of the reactions (like dissolution) between the mineral and surroundings happen on the surface of the mineral grains.

The definition of surface area is not so self-evident. With common sense it could be thought that one estimate for surface area is just the geometric area of sphere. But when looking closerthe surface, it can be understood that the area of sphere assumes that the surface is smooth thus it does not take into account that the surface is not smooth it consists of holes, kinks, etc, see **Figure 10**.

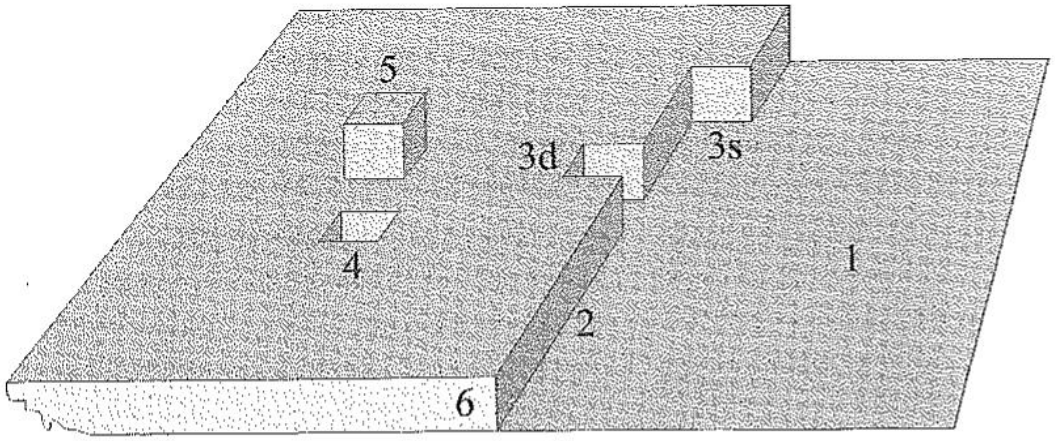

Figure 10 Schematic view of mineral surface; where 1 refers to flat surface, 2 to step, 3 to kink site (3d to double kink site and 3s single kink sit), 4 to hole, 5 to adatom and 6 to corner. The figure is from **[Brantley et al., 2007]**.

When taking into account all the topography of surface the actual surface area enlarges. This surface area is called the total surface area, which can be measured by using BET method **[Brunauer et al., 1938]**.

It should also be noted that the surface may not be similarly reactive; some of the reactions may be more aggressive in corners than on flat surface, meaning that the reactivity of each site varies. In this case the surface area is called as the *reactive surface area*, which is quite difficult to measure and thus use in modelling. All in all surface area measurements for many minerals do not even exist, thus the surface area need to be estimated. In this work the surface areas, see **Table 3**, were taken from **[Xu et al., 2004]**.

More about surface areas can be found from **[Brantley et al., 2007]**, **[Xu et al., 2004]** and **[Wolery & Jarek, 2003]**.

Table 3 The used parameters for surface area calculations. These are from **[Xu et al., 2004]**

Mineral	*Surface area*	*Grain radius*
Primary minerals:		
Albite	9.8	0.001
Cristobalite	9.8	0.001
Gypsum	9.8	0.001
Muscovite	151.6	0.001
Quartz	9.8	0.001
Secondary minerals:		
Brucite	5.0E4	0.001
Gibbsite	5.0E4	0.001
K-feldspar	5.0E4	0.001
Minerals without any data: Ettringite, Friedel_Salt, Hydrotalcite, Katoite, Monosulfoaluminate, Portlandite, Straentlingite, Tobermorite, Tobermorite_14A	5.0E4	0.001
Other minerals (C3AH6, CSH_0.0, CSH_0.4, CSH_0.8, CSH_1.2, CSH_1.667)	assumed at equilibrium	

3.4 Thermodynamic database

The chemical modelling programs consists of two parts: the code and, usually separate file, called database. The database consists of the important thermodynamic parameters which are needed in the code.

The database is usually divided to primary species and secondary species. The difference between these species can be understood by using terms from vector theory. The primary[9] species can be understood as basis vectors and secondary species as all the other vectors; those which can be expressed as linear combination of the basis vectors. This means that the secondary species consists of basis species.

As an example, in **Figure 11** and **12** are few lines from the used database. The database begins, **Figure 11**, with defining the `temperature points`[10] and continues with primary species (`'H2O'`, etc). The first number after the species is species' hydrated radius, second number is the charge number of that species and the third number is species' atomic mass.

After the primary species, there are secondary species **Figure 12**, which are represented on three lines. The first line consists of the name of the secondary species (in this

[9] or often called as basis or master species
[10] temperature points are used later, in context of secondary species

example: `'Ag++'`), its molecular weigh (`107.87`) [g/mol], molar volume (`2.80`) [cm^3/mol], the species electric charge (`2.00`) number of basis species (`4`), and furthermore the stoichiometric coefficients of component (**basis**) species (`-0.5000 'H2O' 0.2500 'O2(aq)' 1.0000 'Ag+' 1.0000 'H+'`).
Thus the reaction of secondary species (`'Ag++'`) looks like:

$$Ag^{++} = -0.5H_2O + 0.25O_2 + Ag^{+} + H^{+}.$$

On the second line there is first the name of the secondary species (`'Ag++'`) and it is followed by the dissociation constants at `temperature points` listed at the beginning of the whole database **Figure 11**. The dissociation coefficients are logK-values in base 10. Furthermore the third line includes again first the name of the species and then it contains regession coefficients (*a, b, c, d, e*) which are used to calculate the log*K* as a function of temperature:

$$\log K = a \ln T_k + b + cT_k + \frac{d}{T_k} + \frac{e}{T_k^2} \qquad (3\text{-}19)$$

where T_k is the temperature in kelvins [K].

After the primary and secondary species, the database continues with describing minerals and gases and is documented in the same way as the secondary species.

More about the thermodynamic database can be found from **[Xu et al., 2004]** and **[Wolery & Jarek, 2003]**.

```
 File format and data suitable for TOUGHREACT V2.3+ (YMP)
 Data converted with deconv2 tool
 from Eq3_thermoddem_lvl1_no-org_26feb08.dat

!end-of-header     Do not remove this record!
'Temperature points:'   8    0.01   25.00   60.00  100.00  150.00  200.00  250.00  300.00
'H2O'                              0.00  0.00     18.015
'H+'                               3.08  1.00      1.008
'O2(aq)'                           0.00  0.00     31.999
'Ag+'                              2.20  1.00    107.870
'Al+++'                            3.33  3.00     26.982


...continues
```

Figure 11. An example of some primary species (‘H2O’, ‘H+’, ‘O2(aq)’, ‘Ag+’ and ‘Al+++’) in database. This is from the beginning of the TOUGHREACT database.

```
...continues

'null'   0.  0.
'Ag++'                     107.870  2.80  2.00    4  -0.5000 'H2O'  0.2500 'O2(aq)'  1.0000 'Ag+'  1.0000 'H+'
'Ag++'                         12.5184   12.1272   11.7177   11.3917   11.1380   11.0143   10.9996   11.0917
'Ag++'                    -0.38530511E+02    0.24919120E+03    0.42779174E-01   -0.11599042E+05    0.76578810E+06

'H2AsO3-'                  124.936  1.81 -1.00    2  -0.5000 'O2(aq)'  1.0000 'H2AsO4-'
'H2AsO3-'                      33.5340   30.5352   27.0342   23.7804   20.5163   17.8878   15.7153   13.8754
'H2AsO3-'                 0.11007853E+02   -0.72997206E+02   -0.12875811E-01    0.14641311E+05   -0.39592789E+06

'AsH3(aq)'                  77.946  0.00  0.00    3  -2.0000 'O2(aq)'  1.0000 'H2AsO4-'  1.0000 'H+'
'AsH3(aq)'                    166.7094  151.8715  134.4823  118.2534  101.8837   88.5985   77.4898   67.8786
'AsH3(aq)'                0.16947188E+03   -0.10904238E+04   -0.17783775E+00    0.11308111E+06   -0.44032735E+07

'Au+++'                    196.967  3.72  3.00    4  -1.0000 'H2O'  0.5000 'O2(aq)'  1.0000 'Au+'  2.0000 'H+'
'Au+++'                         3.4192    4.3563    5.4708    6.5312    7.6431    8.6121    9.5141   10.4153
'Au+++'                   -0.76344074E+02    0.49509100E+03    0.79715899E-01   -0.28637479E+05    0.14689093E+07
...continues
```

Figure 12. An example of some secondary species (‘Ag++’, H2AsO3-‘, ‘AsH3(aq)’ and ‘Au+++’ in database. This is from TOUGHREACT database.

In this work the used database was taken from **[Blanc et al., 2008]**, anyhow that database (THERMODDEM) does not include K-feldspar, which is considered to be quite important in the cement-bentonite interaction **[Savage et al., 2007]** and **[Gaucher & Blanc, 2006]**). In addition the CSH-gels were changed to corresponding from **[Montori et al., 2008]**.

Thus K-feldspar and CSH-gels were added (as secondary species) to the database. The parameters, needed in this database, were taken from **[Montori et al., 2008]** (CSH-gels) and PetraSim's original database (K-feldspar).

Table 4. Parameters for equilibrium constant calculations for CSH-gels (calcium-silicate-hydrates) were taken from **[Montori et al., 2008]** and for K-feldspar from original database (ThermXu.dat) which is attached with PetraSim program. In CSH-gels case: ln K $=f_1 \ln T+f_2+f_3 T+f_4/T+f_5/T^2$ and in k-feldspar case logK $=f_1 \ln T+f_2+f_3 T+f_4/T+f_5/T^2$.

	f_1 or a	*f_2 or b*	*f_3 or c*	*f_4 or d*	*f_5 or e*	*ln K*	*log K*
CSH_0.0	-14.81	95.578	0.01271	-6.470E3	352.73E3	-2.77	-1.20
CSH_0.4	1.8244	-11.59	-666.6E-3	4.8182E3	-2.106E3	14.91	6.48
CSH_0.8	5.7470	-34.87	-330.5E-3	17.550E3	-0.7582E3	56.71	24.63
CSH_1.2	4.0692	-27.42	-30.93E-3	14.229E3	-9.413E3	43.29	18.80
CSH_1.667	4.8947	-34.10	15.46E-3	21.827E3	3.5744E3	67.08	29.13
K-feldspar[11]	-13.2	103	-0.0141	-11.5E3	1.39E6		-0.03

CSH_x, where x is the calcium-to-silica ratio.

In **Appendix B** are listed those parts of the THERMODDEM database, which are used in this model.

[11] The parameters were taken from the original database (ThermXu.dat) where one basis species was replaced: The alo2- was replaced with Al3+. This switching, from one basis species compilation to another, was made by using KSWITCH-program.

3.5 Solution method

Now when we have the tools (equations) to calculate the hydrological and chemical phenomena for the modelled case, we need to concentrate on the solution method.

3.5.1 Flow chart of TOUGHREACT code

The **Figure 13** shows the flow chart of the TOUGHREACT program from that figure it can be seen in which order the needed equations are calculated. This procedure in **Figure 13** is repeated in every block of the model's grid.

In this work those equations which include heat and/or gas flow are not needed thus those parts of the chart have been faded.

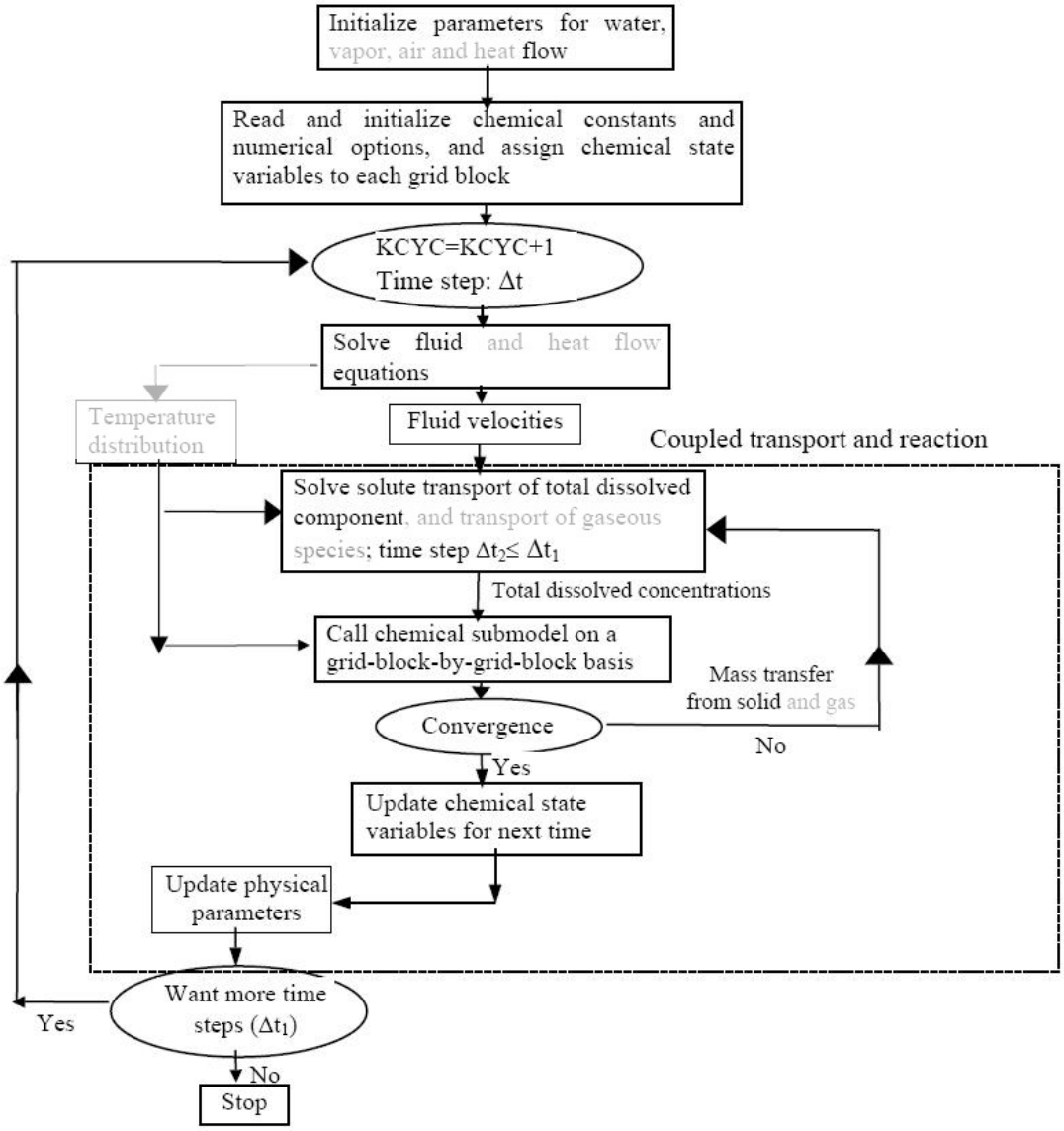

Figure 13. Flow chart of TOUGHREACT program. The parameter KCYC is the time step counter. The parts which are not needed in this work, have been faded. The chart is modified from [Xu et al. , 2004].

The TOUGHREACT solves the equations by using Newton-Raphson method.More about Newton-Raphson method can be found from **[Elden et al. , 2004]**.

4 PRE-CALCULATIONS FOR PETRASIM

4.1 Geometry

The rerangular geometry has been used in the calculation. This is because the interface of PetraSim does not support cylinder geometry[12] thus all cylinder shapes need to be changed to rectangular shapes. In this work it was considered that, when changing the cylinder shape to rectangular form, the area of the inlet end is about equal in both.

Thus the area of cylinder's inlet end

$$A_{\text{experiment}} = A_{\text{cylinder}} = \pi r_{\text{cylinder}}^2 \tag{4-1}$$

where the $r_{cylinder}$ is radius of the cylinder and for rectangular shape the area $A_{rectangular}$ is

$$A_{\text{model}} = A_{\text{rectangular}} = s^2 \tag{4-2}$$

where the s is length of the side at the inlet (and outlet) end of the model.

As mentioned above, in this section, areas of the experiment and the model are the same thus:

$$A_{\text{experiment}} = A_{\text{model}} \Leftrightarrow s = r\sqrt{\pi} \tag{4-3}$$

The radius of the cylinder, used in the experiment, was 0.025 m thus according to **equation (4-2)** the side length of the rectangular in the model is 0.0443 m. The height of the rectangular equals to the height of the cylinder: h = 0.116m.

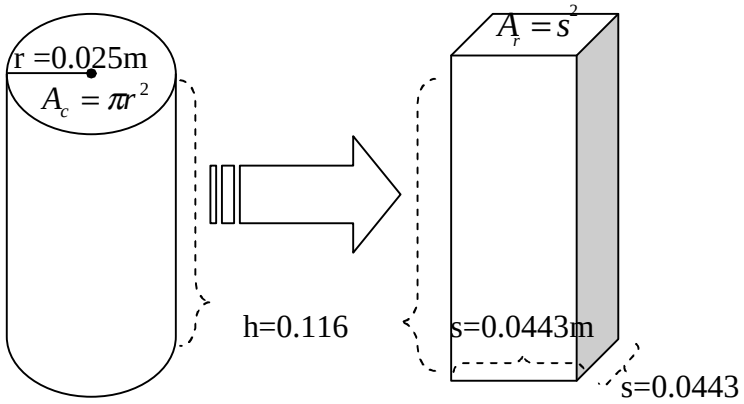

Figure 14. The modelling tool PetraSim does not support the cylinder geometry thus the cylinder used in the experiment is changed to rectangular geometry. The transform was made so that the bottom surface area is equal in the cylinder and the rectangle.

[12] The cylinder shapes can be modelled with TOUGHREACT where AMESH tool is added. In future this feature hopefully will be added to PetraSim.

4.2 Grid

One part of modelling is to generate a grid to the modelled system. In this work the grid is shown in **Figure 15**. Various grids were tested with this modelling case but this was one of those which worked reasonably well: for example, the calculation is interrupted if more vertical lines are added to near the "crushed rock- bentonite"-interface.

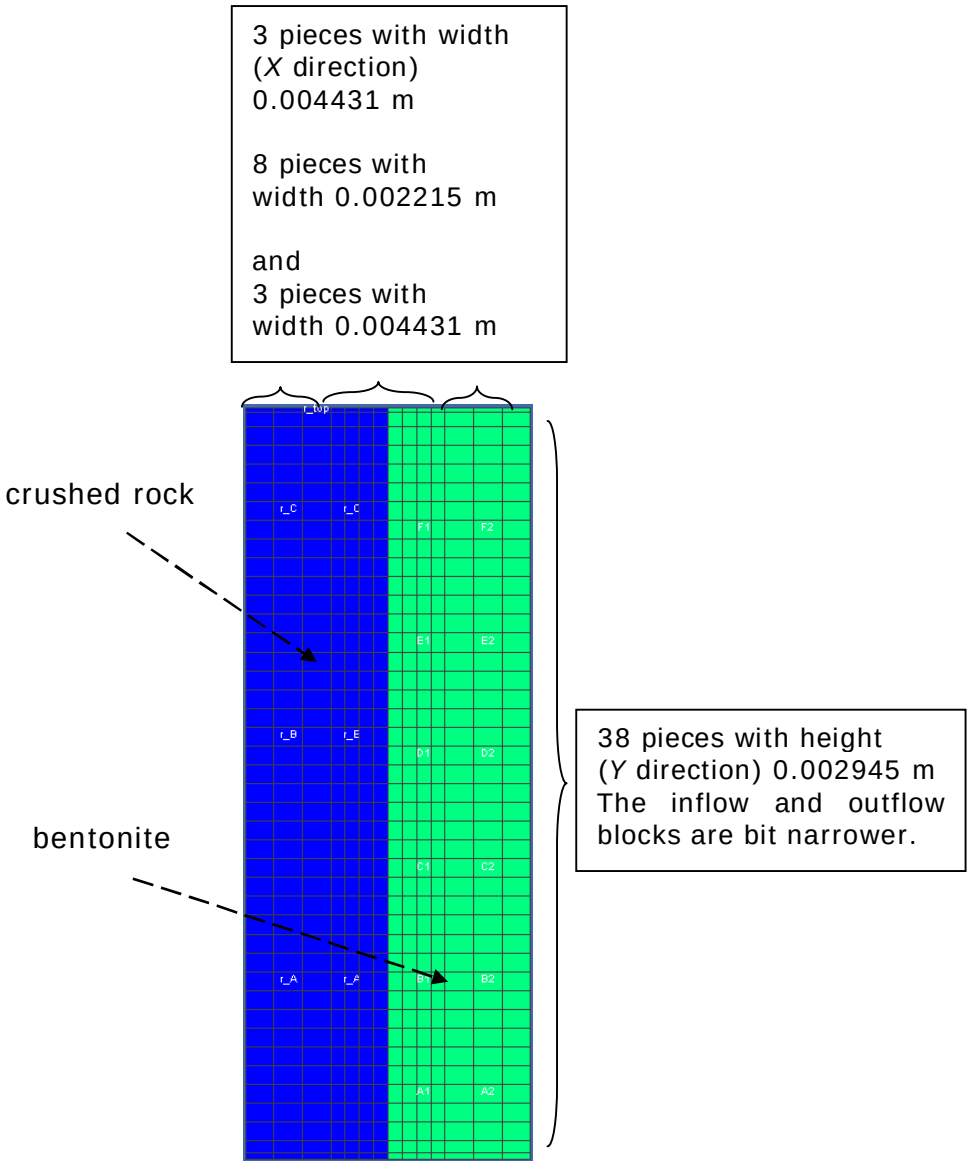

Figure 15. The grid used in the modelling. The crushed rock is on the left hand side (blue area) and bentonite is on the right hand side (turquoise blue area). The grid consisted of 588 grid blocks and the grid elements' width decreases to the interface between these materials. Also the locations, where the "modelling samples" of bentonite (and crushed rock) were taken: these are marked with white letters A1, A2, …, F1, F2. Compare these letters to the **Figure 3.**

4.3 Flow rate in the grid blocks

As seen from **Figure 2** the inflow velocity is 2.5 mL / day. First of all in PetraSim the units need to be changed to kg/s. Thus 2.5 mL / day is $28.9 \cdot 10^{-9}$ kg/s. Furthermore in PetraSim this kg/s needs to be divided between the grid blocks **Figure 15**. Thus with

this grid the inflow (and outflow) velocities are calculated to be $2.89 \cdot 10^{-9}$ kg/s in the narrower grid blocks and $5.79 \cdot 10^{-9}$kg/s in the wider blocks in the inflow (and outflow) end.

The flow velocities were calculated in the following way:

$$\frac{28.9 \cdot 10^{-9}\,\text{kg/s}}{5} = 5.79 \cdot 10^{-9}\,\text{kg/s}$$

And for narrower blocks this is still divided by two.

$$\frac{5.79 \cdot 10^{-9}\,\text{kg/s}}{2} = 2.89 \cdot 10^{-9}\,\text{kg/s}$$

The flow rate needs to be equal in both the inflow and outflow ends; otherwise the pressure will rise in the cylinder.

4.4 Minerals

As mentioned before, the bentonite is not a mineral but a set of minerals. In the experiment the mineral composition of bentonite was measured by using XRD analysing, the results are seen in **Table 5**.

In the experimental results the mineral composition is presented as mass fractions, whereas in PetraSim the mineral composition should be presented in volume fractions. Thus there is a need for few pre-calculation; with simple, volume equals to mass divided by density of the mineral (**equation (4-4)**), the mass fractions were changed to volume fractions.

$$\rho = \frac{m}{V} \Leftrightarrow V = \frac{m}{\rho} \tag{4-4}$$

In the experiment the other half of the cylinder was filled up with 194.4g bentonite, from which 8% were water, thus the actual amount of bentonite (m_b) were 178.9g. From the mass fractions the amount for each mineral were calculated according to **equation (4-5)**.

$$m_\beta = X_\beta^\kappa m_{\text{bentonite}} \tag{4-5}$$

where the β indicates the mineral (montmorillonite, albite,... etc) and X_β^κ is the mass fraction of the mineral.

In **equation (4-4)** there is also need for density of the mineral. These densities for each mineral were collected from Mineralogy Database **[Barthelmy , 2008]**.

Table 5. The mineral composition of the bentonite in this work.

	Mineral	*Mass fraction* X_β^k (**)	*Density* ρ_β *[g/cm³]* (***)	*Mass* m_β *[g]* $m_\beta = X_\beta^k m_{bento}$	*Volume [cm³]* $V_\beta = m_\beta / \rho_\beta$	*Volume fraction*
Bentonite	Cation exchanger (montmorillonite) (*)	0.83	2.8	148.47	53.03	0.82
	Albite	0.07	2.62	12.52	4.78	0.07
	Cristobalite	0.05	2.27	5.37	2.36	0.04
	Gypsum	0.03	2.3	1.79	0.78	0.01
	Muscovite	0.01	2.82	1.79	0.63	0.01
	Quartz	0.01	2.62	8944	3.41	0.05
Sum		1		178.88	64.99	1

(*) Note that montmorillonite is not added into PetraSim as a mineral because it is treated as an cation exchanger rather than mineral.
(**) From [**Vuorinen et al. , 2006]**
(***) From **[Barthelmy , 2008]**

It should also be noted that in PetraSim there is also an option to volume fraction for *secondary species* (even though these are not present at the beginning of the model). In PetraSim this value is **1.0** by default but the user should change it to something more reasonable, like in this work 10^{-6}.

4.5 Porosity

As described above in **equation (3-6)** the porosity is defined to be the volume of empty space divided by total volume. In this case there are of course two porosities which need to be calculated; one for the bentonite and one for the crushed rock.

The total volume for both cases is quite easy to calculate: it is half of the cylinder's volume:

$$V_{\text{total}} = V_{½} = \frac{1}{2}\pi r^2 h = \frac{1}{2}\pi\left(2.5\text{cm}\right)^2 11.78\text{cm} = 115.6\text{cm}^3 \qquad (4\text{-}6)$$

4.5.1 Porosity of bentonite

It can be seen from **Table 5** that the volume of bentonite $V_{\text{bentonite}}$ is 64.99cm^2. Thus the porosity for bentonite is

$$\phi_{\text{bentonite}} = 1 - \frac{V_{\text{bentonite}}}{V_{\text{total}}} = 1 - \frac{64.994\text{cm}^3}{115.65\text{cm}^3} = 0.438 \qquad (4\text{-}7)$$

4.5.2 Porosity of crushed rock

The density of crushed rock is 2.65g/cm^3 and according to the experiment there were 219.1g crushed rock thus the volume for crushed rock is

$$\rho_{\text{crushed rock}} = \frac{m_{\text{crushed rock}}}{V_{\text{crushed rock}}} \Leftrightarrow V_{\text{crushed rock}} = \frac{m_{\text{crushed rock}}}{\rho_{\text{crushed rock}}} = \frac{219.1\text{g}}{2.65\text{g/cm}^3} \approx 82.7\text{cm}^3 \qquad (4\text{-}8)$$

Therefore the porosity for crushed rock is

$$\varphi = 1 - \frac{V_{\text{crushed rock}}}{V_{\text{total}}} = 1 - \frac{82.7\text{cm}^3}{115.65\text{cm}^3} \approx 0.285 \qquad (4\text{-}9)$$

4.6 Tortuosity

The tortuosity of material is an empirical quantity, thus it is defined separately for bentonite and crushed rock.

4.6.1 Tortuosity for bentonite

In TOUGH2 the effective diffusivity is defined as

$$D_{\text{e}} = \varphi \tau D_{\text{w}} \qquad (4\text{-}10)$$

where φ is the porosity, τ is tortuosity and D_w is the free water diffusivity $2.27 \cdot 10^{-9}$m^2/s.

Thus the equation for tortuosity is

$$\tau = \frac{D_{\text{e}}}{\phi D_{\text{w}}} \qquad (4\text{-}11)$$

Figure 16 is from **[Ochs & Talerico, 2004]** and from that figure it can be seen that the effective diffusion coefficient D_e, for bentonite with dry density 1 540 kg/m^3, is $1.3 \cdot 10^{-10}$m^2/s.

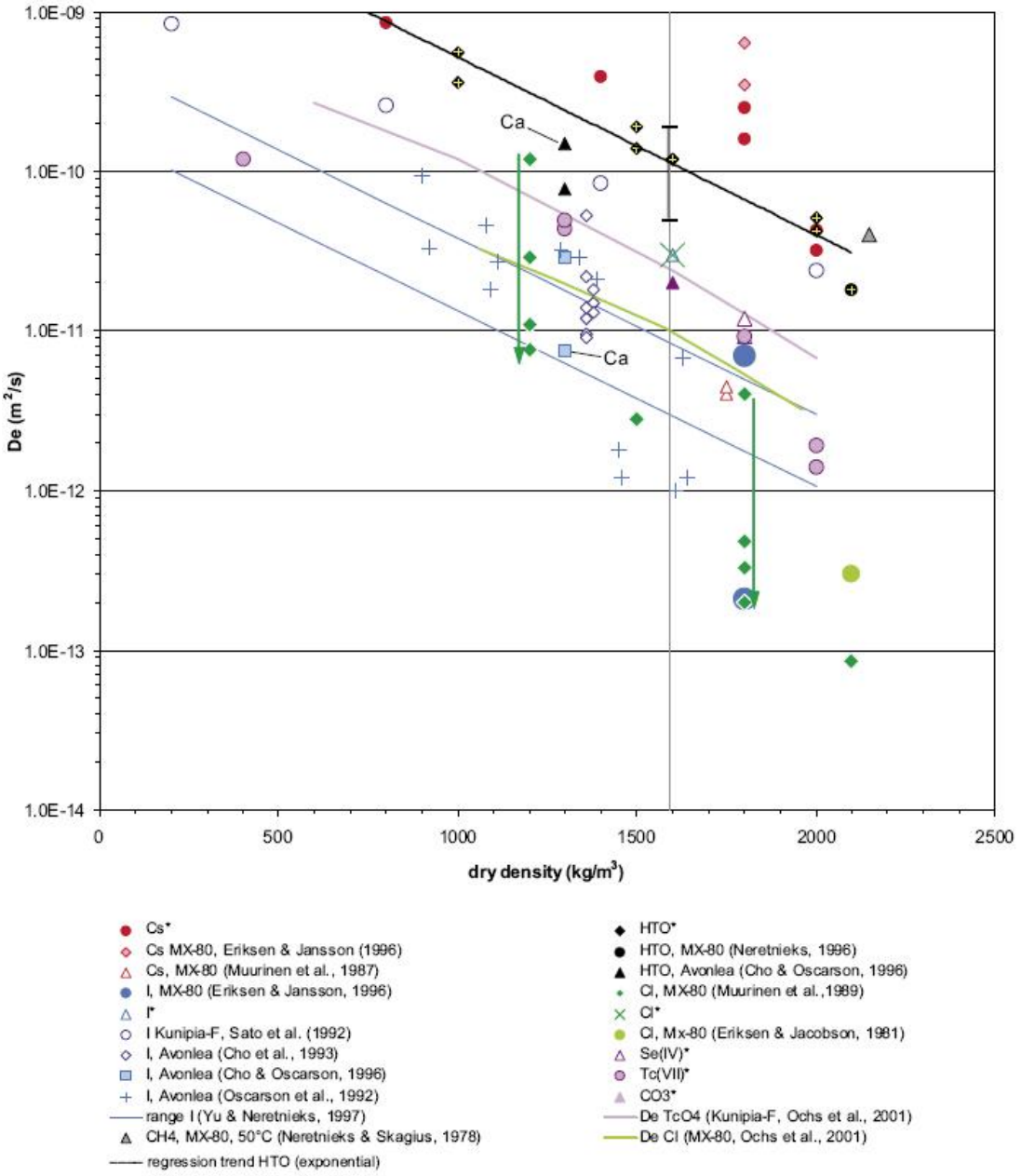

Figure 16. Plot of effective diffusivities fos Cs, HTO and various anions as a function of dry density, from **[Ochs & Talerico , 2004]**. In this work the interest is on diffusivity of HTO* at bentonite's dry density 1 540 kg/m^3.

Thus the value used for bentonite's tortuosity is

$$\tau_{\text{bento}} = \frac{D_e}{\varphi\, D_w} = \frac{1.3 \cdot 10^{-10}\, m^2/s}{0.438 \cdot 2.27 \cdot 10^{-9}\, m^2/s} \approx 0.13 \qquad (4\text{-}12)$$

4.6.2 Tortuosity for crushed rock

The effective diffusion coefficient for crushed rock can be calculated by using Bruggeman's equation:

$$D_e = \varphi^{3/2} D_w \tag{4-13}$$

in TOUGHREACT the effective diffusion is as in **equation (4-10)** thus adding **equations (4-11)** and **equation (4-13)** it gives:

$$\tau = \varphi^{1/2} = \sqrt{0.285} \approx 0.53 \tag{4-14}$$

4.7 Permeability

The permeability parameter in **equation (3-4)** need to be defined for both bentonite and crushed rock.

4.7.1 Permeability for bentonite

The permeability for bentonite has been taken from **[Harrington & Horseman, 2003]** which suggest that bentonite with dry density 1 600 kg/m^3 has permeability of $1.0 \cdot 10^{-21}$ m^2. Similar values to permeability can be found from **[Jussila, 2007]** thus this value has been used in the model.

4.7.2 Permeability for crushed rock

The permeability for crushed rock has been calculated by using **equation (4-15) [Odong, 2007]**

$$C = \frac{k \cdot g}{\upsilon} \tag{4-15}$$

where C is conductivity of water (40-60 m/day **[Odong, 2007]**), k is permeability, g is acceleration due to gravity 9.81 m/s^2 and υ is kinematic viscosity of water ($9.0 \cdot 10^{-7}$m^2/s, 25 ºC**[The Engineering ToolBox, 2005]**).

After rearranging and calculating the **equation (4-15)** we get

$$k = \frac{C \cdot \upsilon}{g} = \frac{\frac{50m}{24 \cdot 60 \cdot 60s} \cdot 9.0 \cdot 10^{-7}\, m/s}{9.81 m/s^2} \approx 5.0 \cdot 10^{-11} m^2 \tag{4-16}$$

thus it is reasonable to use permeability $5.0 \cdot 10^{-11}$m^2 for crushed rock.

4.8 Pre-calculations for cation exchange

In the experiment **[Vuorinen et al., 2006]** one aim was to study the cation exchange processes in the montmorillonite. Therefore the cation exchange parameters of montmorillonite were measured before and after the experiment.

To model the cation exchange processes of this experiment, there are at least three different pre-calculations which need to be calculated. The first calculation concerns the equivalent fraction. The second calculation corrects one bug found from TOUGHREACT (and thus from PetraSim) and the third calculation was done to initialize the cation exchanger so that it corresponds to the montmorillonite's (used in the experiment) cation exchange properties.

4.8.1 Calculating the equivalent fractions

The equivalent fractions are calculated because they are needed when defining the initial water for bentonite, see **chapter 4.8.3**.

In the experiment the exchangeable cations was determined by NH_4-CEC and the cation exchange capacity (CEC) by using Cu-CEC. The results are collected in **Table 6**.

Table 6 shows also the average values of the experimental results and the corresponding equivalent fractions. As an example of equivalent fraction calculation for calcium is:

$$\beta_{CaX} = \frac{0.106}{0.717} = 0.148 \tag{4-17}$$

Table 6. The data for calculating the equivalent fractions[Vuorinen et al. , 2006].

	Ca	K	Mg	Na	SUM (i.e the CEC)
meq/g	0.106	0.0086	0.0502	0.552	0.717
Equivalent fraction [b)]	0.148	0.0120	0.0700	0.770	1

4.8.2 Bug in cation exchange in TOUGHREACT

During this work it was found out that the PetraSim does not calculate the cation exchange properties the way it is promised in TOUGHREACT manual.

In manual it is said that the concentration of the *i*-th exchanged cation w_j (in moles per liter of fluid) can be obtained from the i-th equivalent fraction:

$$w_j = \beta_j \mathrm{CEC} \rho_s \frac{(1-\phi)}{100 \phi z_j} \tag{4-18}$$

where the β_j is the equivalent fraction, CEC is the cation exchange capacity, ρ_s is the solid's density, φ is the porosity and z_j is the charge of the cation.
It was found that TOUGHREACT calculates according to **equation (4-18)** only if the density of modelled mineral is 2.65 g/cm^3. In this work the modelled material, bentonite, does not have density of 2.65 g/cm^3 but 2.75 g/cm^3.

After discussion with the developer of TOUGHREACT it was found that this problem can be circumvented by the following equation:

$$CEC_{\text{input}} = CEC_{\text{experiment}} \frac{\rho_{\text{material}}}{\rho_{\text{default}}} = CEC_{\text{experiment}} \frac{\rho_{\text{material}}}{2.65\,{}^{\text{g}}\!/\!_{\text{cm}^3}} \tag{4-19}$$

where the CEC_{input} is the modified cation exchange capacity, $CEC_{\text{experiment}}$ is the cation exchange capacity from the experiment (in this case 74 meq/100g), ρ_{default} is the fixed solid density 2.65 g/cm^3 and ρ_{material} is the density of the modelled material.

Thus in this work the input cation exchange capacity is

$$CEC_{input} = 71.7\,{}^{meq}\!/\!_{100g} \cdot \frac{2.75\,{}^{g}\!/\!_{cm^3}}{2.65\,{}^{g}\!/\!_{cm^3}} = 74.4\,{}^{meq}\!/\!_{100g} \tag{4-20}$$

4.8.3 Initialising the cation exchanger

The composition of bentonite's porewater is largely studied but still quite unknown. Anyhow in the modelling work there is a need for at least some kind of porewater composition.

In this work it has been considered that the porewater composition can be calculated from the cation exchanger composition. The exchanger (which is montmorillonite) composition, regarding the major cations is known from the experiment, thus the porewater can be thought as an "image" of the cation exchanger.

The major cations in this case are Na^+, Ca^{2+}, K^+ and Mg^{2+} and the cation exchange equations are:

$$2NaX + Ca^{2+} \Leftrightarrow CaX_2 + 2Na^+ \qquad K^{Na/Ca} \qquad \text{Reaction 3}$$

$$2NaX + Mg^{2+} \Leftrightarrow MgX_2 + 2Na^+ \qquad K^{Na/Mg} \qquad \text{Reaction 4}$$

$$NaX + K^+ \Leftrightarrow KX + Na^+ \qquad K^{Na/K} \qquad \text{Reaction 5}$$

where the X^- means one mole of cation exchanger, in this case montmorillonite.

The equilibrium constants for these reactions are by definition, **equation (3-12)**:

$$K^{Na/Ca} = \frac{\{CaX_2\}\{Na^+\}^2}{\{NaX\}^2\{Ca^{2+}\}} = \frac{\{CaX_2\}\{\gamma_{Na^+}[Na^+]\}^2}{\{NaX\}^2\{\gamma_{Ca^{2+}}[Ca^{2+}]\}} = \frac{\beta_{CaX_2}\ \gamma^2_{Na^+}[Na^+]^2}{\beta_{NaX}\ \gamma_{Ca^{2+}}[Ca^{2+}]} \quad (4\text{-}21)$$

$$K^{Na/Mg} = \frac{\beta_{MgX_2}\ \gamma^2_{Na+}[Na^+]^2}{\beta_{NaX}\ \gamma_{Mg^{2+}}[Mg^{2+}]} \quad (4\text{-}22)$$

$$K^{Na/K} = \frac{\beta_{KX}\gamma_{Na^+}[Na^+]}{\beta_{NaX}\gamma_{K^+}[K^+]} \quad (4\text{-}23)$$

In this modelling case the values for $K_{Na/I}$ are calculated according to the Gaines-Thomas convention **[Bradbury & Baeyens, 2003]** and the β_{NaX} are determined in the experimental work **[Vuorinen et al., 2006]**.

Because the aim was to calculate the porewater composition, **equations (4-21)**, **(4-22)** and **(4-23)** need to be rearranged so that the concentrations of major cations can be calculated. Thus

$$[Ca^{2+}] = \frac{\beta_{CaX_2}}{\beta_{NaX}} \cdot \frac{\gamma^2_{Na^+}}{\gamma_{Ca^{2+}}} \cdot \frac{[Na^+]^2}{K^{Na/Ca}} \quad (4\text{-}24)$$

$$[Mg^{2+}] = \frac{\beta_{MgX_2}}{\beta^2_{NaX}} \cdot \frac{\gamma^2_{Na^+}}{\gamma_{Mg^{2+}}} \cdot \frac{[Na^+]^2}{K^{Na/Mg}} \quad (4\text{-}25)$$

$$[K^+] = \frac{\beta_{KX}}{\beta_{NaX}} \cdot \frac{\gamma_{Na+}}{\gamma_{K+}} \cdot \frac{[Na^+]}{K^{Na/K}} \quad (4\text{-}26)$$

In this kind of chemical environment it is also important to be sure that the electrical balance is neutral, thus the concentration of chloride is calculated by assuming that there are as many anions (Cl^-) as major cations. Thus

$$[Cl^-] = 2\cdot[Ca^{2+}] + 2\cdot[Mg^{2+}] + [Na^+] + [K^+]$$
$$= 2\cdot\left(\frac{\beta_{CaX_2}}{\beta_{NaX}} \cdot \frac{\gamma^2_{Na^+}}{\gamma_{Ca^{2+}}} \cdot \frac{1}{K^{Na/Ca}} + \frac{\beta_{MgX_2}}{\beta_{NaX}} \cdot \frac{\gamma^2_{Na+}}{\gamma_{Mg^{2+}}} \cdot \frac{1}{K^{Na/Mg}}\right)[Na^+]^2 + \left(\frac{\beta_{KX}}{\beta_{NaX}} * \frac{\gamma_{Na+}}{\gamma_{K+}} * \frac{1}{K^{Na/K}} + 1\right)[Na^+] \quad (4\text{-}27)$$

and after rearranging the **equation (4-27)** we get

$$2\cdot\frac{\gamma_{\mathrm{Na+}}^2}{\beta_{\mathrm{NaX}}}\left(\frac{\beta_{CaX_2}}{\gamma_{\mathrm{Ca^{2+}}}\cdot K^{\mathrm{Na}/\mathrm{Ca}}}+\frac{\beta_{\mathrm{MgX_2}}}{\gamma_{\mathrm{Mg^{2+}}}\cdot K^{\mathrm{Na}/\mathrm{Mg}}}\right)\left[\mathrm{Na^+}\right]^2+\left(\frac{\beta_{\mathrm{KX}}}{\beta_{\mathrm{NaX}}}\cdot\frac{\gamma_{\mathrm{Na+}}}{\gamma_{\mathrm{K+}}}\cdot\frac{1}{K^{\mathrm{Na}/\mathrm{K}}}+1\right)\left[\mathrm{Na^+}\right]-\left[\mathrm{Cl^-}\right]=0 \quad (4\text{-}28)$$

which is quadratic equation $ax^2+bx+c=0$, with x= [Na^+] where

$$a=2\cdot\frac{\gamma_{\mathrm{Na+}}^2}{\beta_{\mathrm{NaX}}}\left(\frac{\beta_{CaX_2}}{\gamma_{\mathrm{Ca^{2+}}}\cdot K^{\mathrm{Na}/\mathrm{Ca}}}+\frac{\beta_{\mathrm{MgX_2}}}{\gamma_{\mathrm{Mg^{2+}}}\cdot K^{\mathrm{Na}/\mathrm{Mg}}}\right),$$

$$b=\left(\frac{\beta_{\mathrm{KX}}}{\beta_{\mathrm{NaX}}}\cdot\frac{\gamma_{\mathrm{Na+}}}{\gamma_{\mathrm{K+}}}\cdot\frac{1}{K^{\mathrm{Na}/\mathrm{K}}}+1\right)$$

and

$$c=-\left[\mathrm{Cl^-}\right]$$

thus the concentration of Na^+ can be solved by using the quadratic equation solver. This "image" idea has been presented more detailed in **[Tournassat et al., 2007]**.

The parameters for cation exchanger have been measured in the experiment.

Table 7. The relevant parameters for cation exchange phenomena.

Parameter	*Unit / Reaction*	*Value*
$\log K_{Na/K}$	$K^+ + NaX \Leftrightarrow KX + Na^+$	0.6 [a]
$\log K_{Na/Ca}$	$Ca^{2+} + 2NaX \Leftrightarrow CaX_2 + 2Na^+$	0.41 [a]
$\log K_{Na/Mg}$	$Mg^{2+} + 2NaX \Leftrightarrow MgX_2 + 2Na^+$	0.34 [a]
CEC	meq / 100 g	0.72 [b]
Initial NaX	(equivalent fraction)	0.77 [b]
Initial KX	(equilvalent fraction)	0.01 [b]
Initial Ca_2X	(equivalent fraction)	0.15 [b]
Initial Mg_2X	(equivalent fraction)	0.07 [b]

[a] from **[Bradbury & Baeyens , 2003]**
[b] from the experiment

By solving the **equations (4-24) – (4-27)** and by using parameters from **Table 7** we get an estimated porewater composition which is used as an initial water in PetraSim. This initial water composition is shown in **Table 8.**

Table 8. Composition of initial water, by using results from experiment **[Vuorinen et al. , 2006]** and equations from **[Tournassat et al. , 2007]**. *NOTE that this is not the inflow water.*

species	*mol/l*
$[Na^+]$	10.0E-06
$[K^+]$	39.0E-09
$[Ca^{2+}]$	9.7E-12
$[Mg^{2+}]$	5.4E-12
$[Cl^-]$	10.0E-6

When using water with this composition **Table 8** and equilibrium constants *K* from **Table 7** the cation exchanger (montmorillonite) should be filled with cation distribution described in **Table 7**.

5 RESULTS

The model's pH resuls are taken from grid block r_top, see **Figure 17** and the cation exchange results (at selected times) are from the grid blocks, which are coloured as yellow.

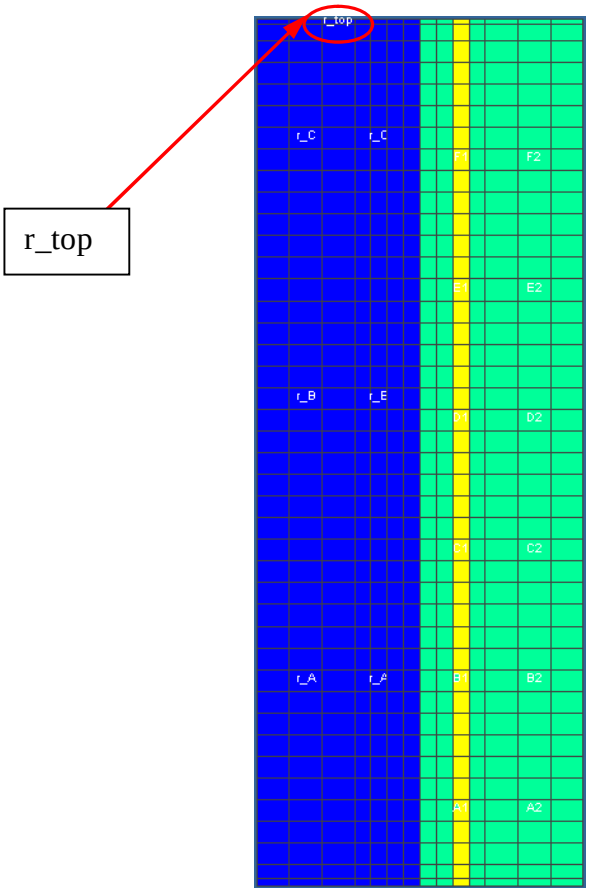

Figure 17. The areas where the results are taken. The pH results are taken from grid block which is named as r_top and the cation exchange results are taken from the area which is coloured with yellow.

5.1 The cation exchange

The cation exchange capacities (CEC) were measured in the experiment for every master species (Na^+, Ca^{2+}, K^+ and Mg^{2+}). The results from the experiment can be seen from **Figure 18** and **Figure 19**. The same figures show also the modelled results.

The results from the experiment are on the left hand side and results from the model are on the right hand side.

The modelling program PetraSim does not print out the amount of cations in eq/g thus some post-calculations were done before the **Figures 18** and **19** could be drawn. These precalculations are presented in **Appendix E**.

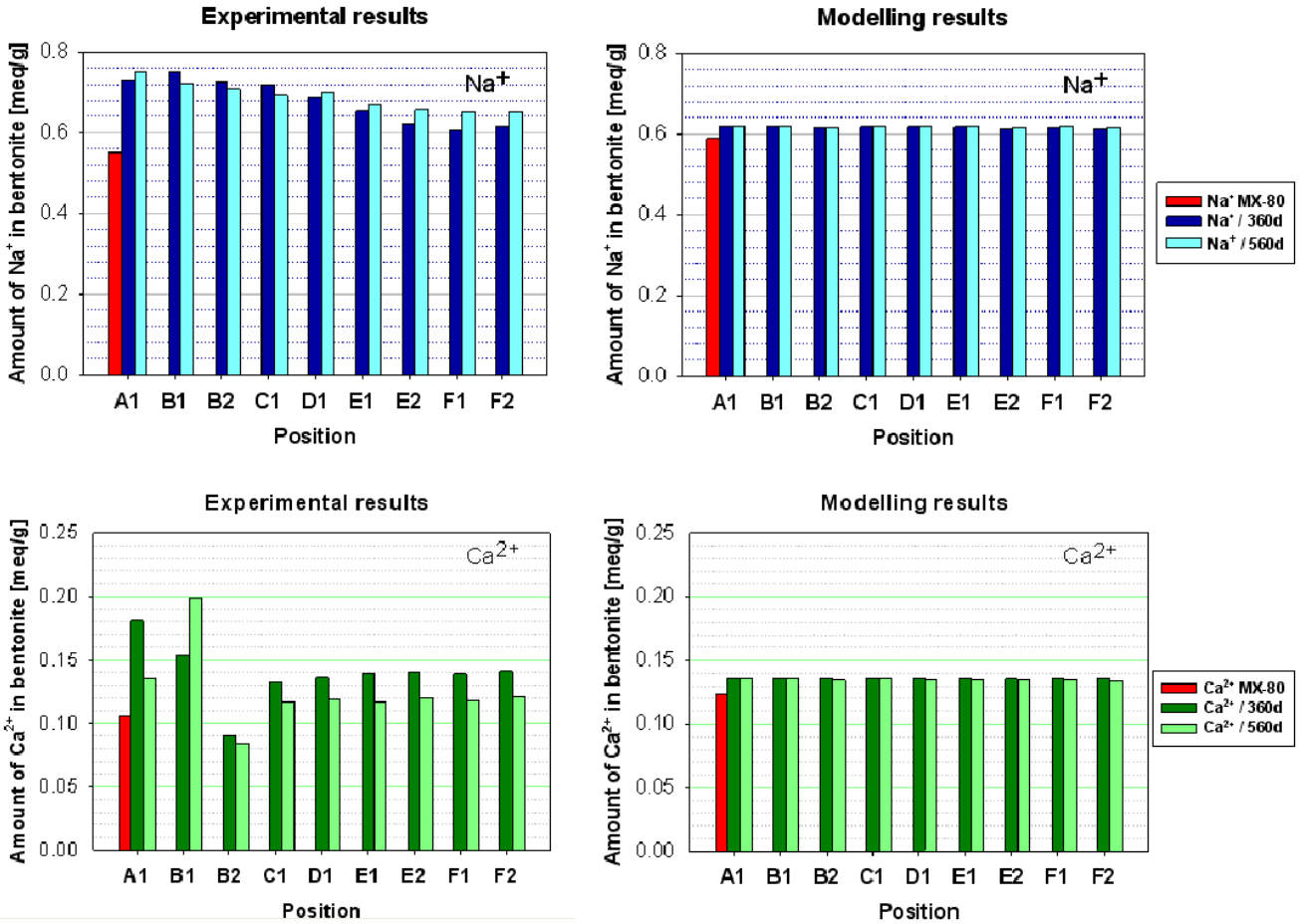

Figure 18. The cations in bentonite. On the left hand side are the measured CEC values [meq/g] and on the right hand side are the results [mol/L] from the modelling. The pictures are not meant to present the quantitative amount of cation but qualitative behaviour. This is because the PetraSim does not calculate CEC values, only concentrations. The alphabets refer to **Figure 3**: A indicates the in-flow end of the experiment and F the out-flow end.

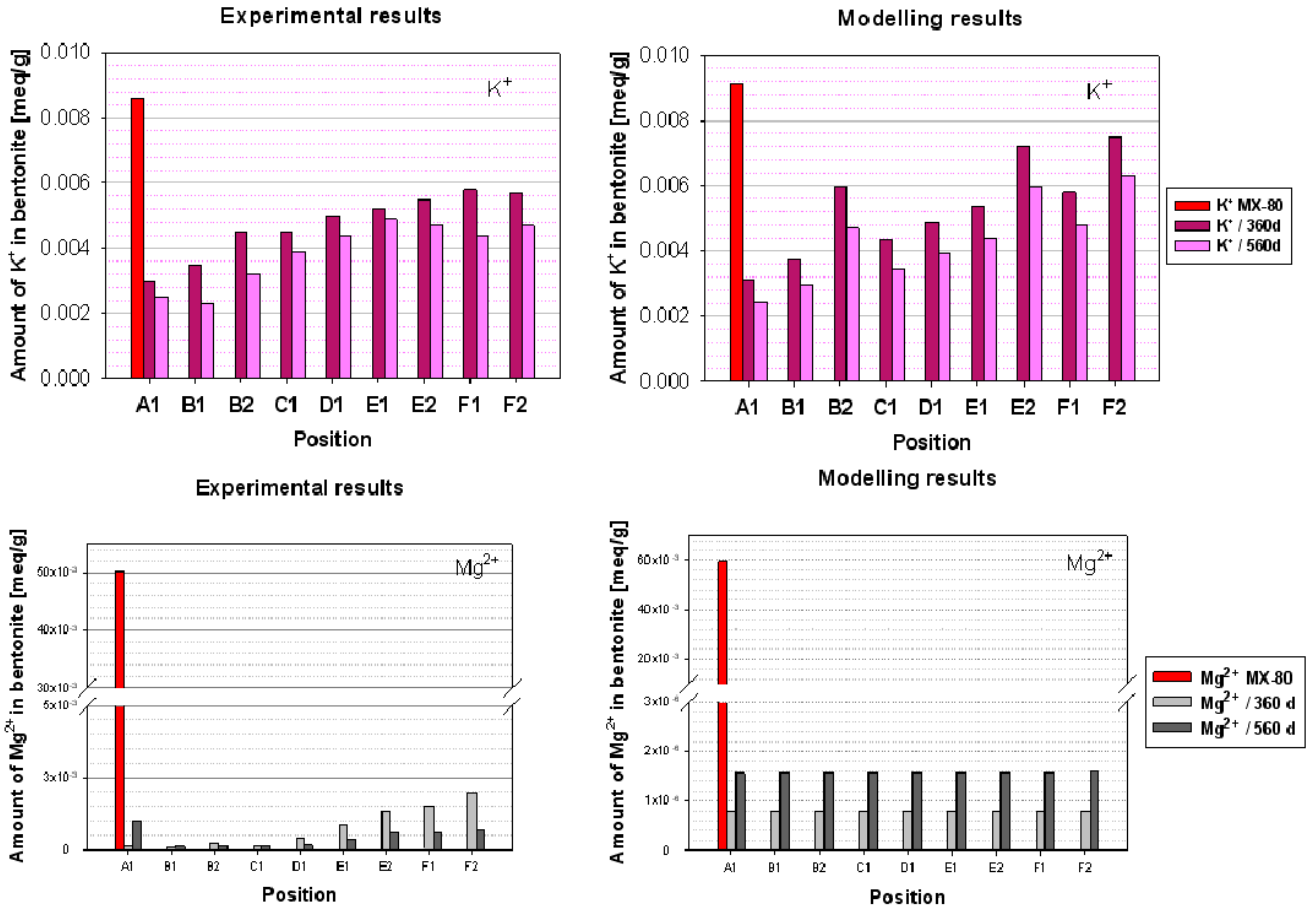

Figure 19. The cations in bentonite. On the left hand side are the measured CEC values [meq/g] and on the right hand side are the results [mol/g] from modelling. The alphabets on x-axis refer to **Figure 3**: A indicates the in-flow end of the experiment and F the out-flow end. *Note*, in the Mg^{2+} case, that modelling results are $*10^{-6}$ [mol / L], and also that there is a break in y-axis.

5.2 pH outlet

In the experiment there was also interest on the pH of the outflow water. **Figure 20** shows the evolution of the pH as a function of time. On the left hand side there are results from the experiment and on the right hand side are the modelled results.

It should be noted that with PetraSim it is not possible to get the composition of the outflow water but it is possible to define the pH near the outlet end. The model results in **Figure 20** were calculated from the r_top grid block, see **Figure 15**.

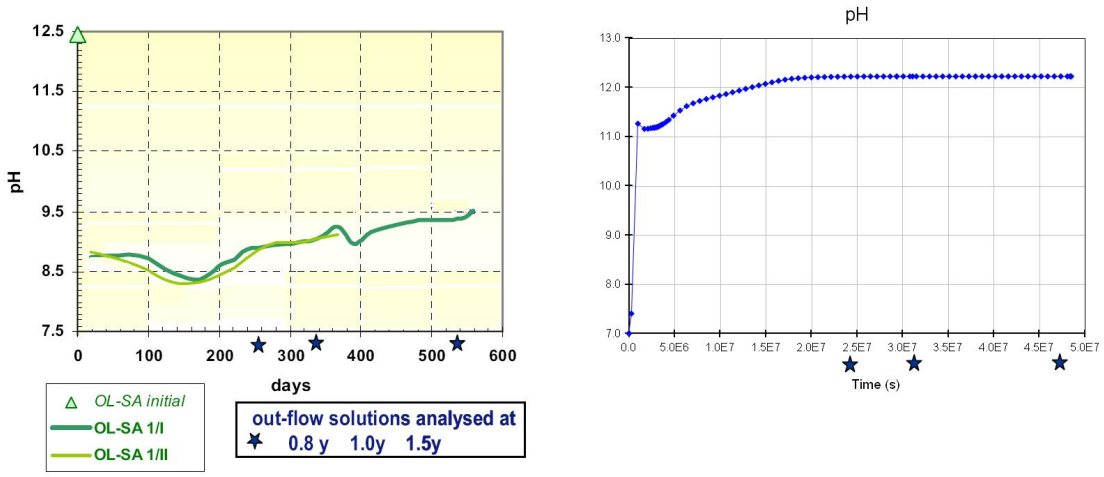

Figure 20. The evolution of pH; results from the experiment are on the left hand side and results from the modeling are on the right hand side. Note the scales in the figures. On the left hand side the time is in ohurs whereas in the right hand side in seconds. The figure is left this way because of the poor output format of TOUGHREACT.

5.3 Mineral transformation

In the ECOCLAY experiment the mineral composition at the end of the experiment was not defined. Only the composition at the beginning was determined see **Table 5**.

However after the experiment, when the cylinders were opened, it was noticed that the endings of the cylinder and the interface of bentonite and crushed rock were slimy which was assumed to mean formation of new phases. Nevertheless, as mentioned, these possible new phases were not specified.

In the modelling work one interest was thus in these new phases: what would these be? The modelling results are collected in **Figure 21**. In **Figure 21** there is the mineral composition of the bentonite at the beginning of the model on the left hand side; and after 560 days on the right hand side.

The upper row of the figures shows the whole distribution of minerals but because the alterations were so small the same figures were “zoomed” and these “zoomed” figures are in the lower row.

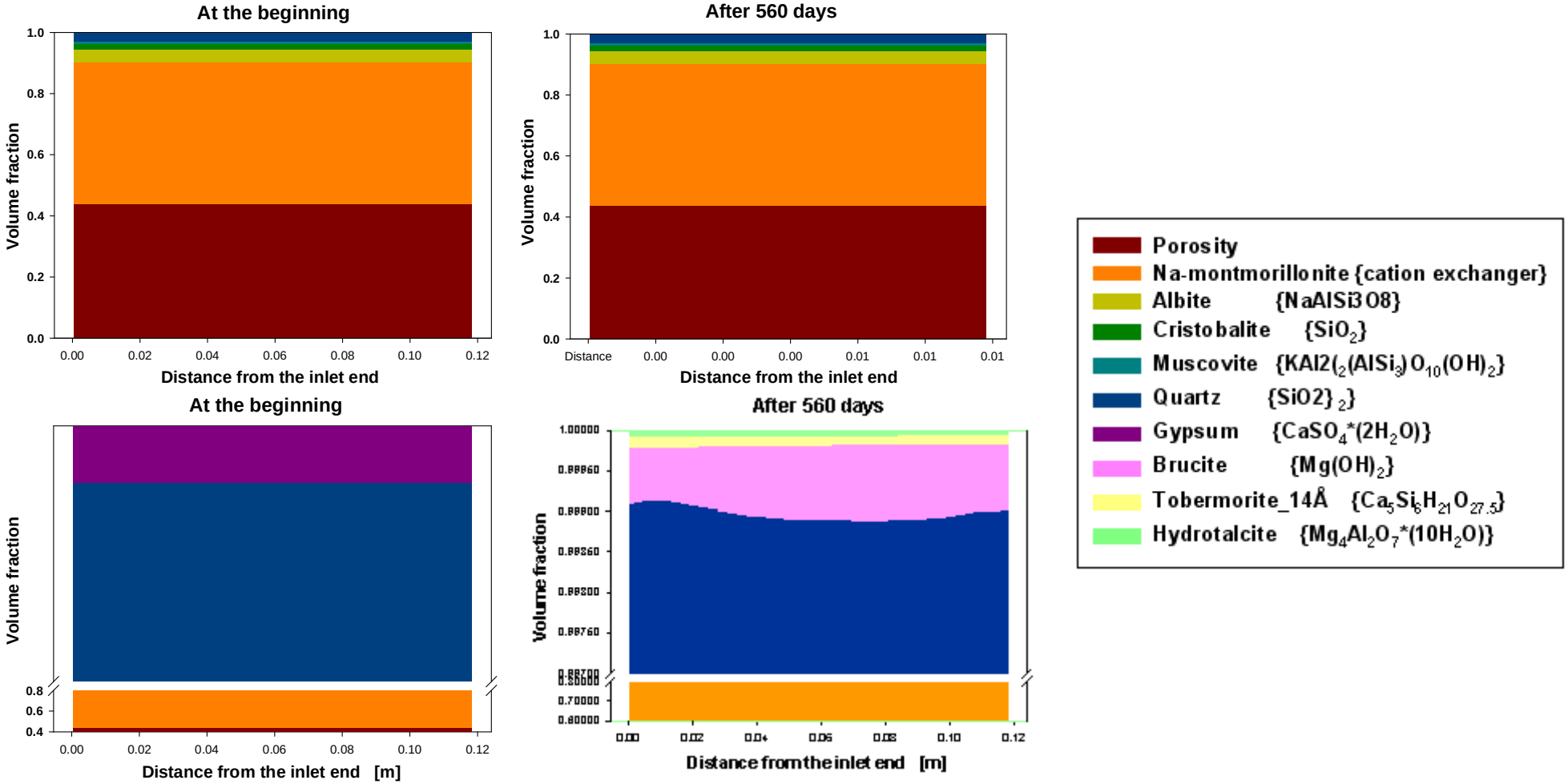

Figure 21. The mineral evolution of bentonite: at the beginning of the experiment (on the right hand side) and at the end of the experiment (on the left hand side. The lower figures are only zoomed version of figures above, where the y-axis has break from point y = 0.8 to point y= 0.997.

6 DISCUSSION

6.1 Cation exchange

When comparing the modelling results to those from experiment, see **Figure 18** and **Figure 19**, it can be seen that cations seems to correspond each quite nicely. Only the Mg^{2+} ion has clear difference between the experiment and the model. In model the amount of equivalents is lesser than in the experiment.

The selectivity coefficients in **Table 7** suggest that the initial sodium in cation exchanger would be replaced by calcium. Though, from the **Figure 18** it can be seen that in this experiment the sodium in cation exchanger is not replaced by calcium. This is because the inflow water (see **Table 1**) includes much sodium instead of calcium.

6.2 Evolution of outlet pH

The results from the experiment and the model do not coincide at all. First it should be noted, as said in previous chapter, that the outflow composition can not be modelled with the program used and thus the pH results from modelling can not be directly compared to the experimental results.

Though, similar trend with the modelled and experimental results, were assumed to be seen. However in the experiment the pH levelled off from 12.5 to near 9 whereas in the model the pH increases from the initial pH 7 up to 12.5.

In the experiment this significant pH drop was considered to be due to bentonite's character to buffer pH.

One reason for this difference could be that in montmorillonite theory it is considered that the montmorillonite consists of thin sheets and the montmorillonite's pH buffer character is partly based on the surface hydroxyl sites (≡SOH) at the end of sheets: these surface hydroxyl sites can protonate ($\equiv SOH_2^+$) or deprotonate ($\equiv SO^-$), depending on the solution pH **[Metcalfe & Walker, 2004]**.

Anyhow PetraSim is not able to handle the interaction between montmorillonite and surface hydroxyl sites. To model this interaction with PetraSim, the program should have the capability to use surface complex-model. The lack of surface complex-model is probably one reason why the model results of pH evolution do not coincide with the experiment.

In montmorillonite theory it has also been noted that montmorillonite's pH buffer capacity is also caused by the montmorillonite lattice itself, this is because the montmorillonite is dissolving by **Reaction 6**.

$$\text{Na-montmorillonite} + 6H_2O + 4.67OH^- \rightarrow \text{reaction products} \qquad \text{Reaction 6}$$

which means that one mole of Na-montmorillonite consumes 4.67 moles of OH^-. Meaning that the theoretical montmorillonite's buffering capacity is 12.7 moles of OH^- per one kilogram of montmorillonite **[Savage & Benbow, 2007]**.

In *this model* though, the montmorillonite does not dissolve and thus that dissolving phenomena does not buffer the pH in this work.

This was a selection and it was made because PetraSim does not couple the dissolving of montmorillonite and the cation exchange capacity (CEC). This means, that if montmorillonite with volume fraction 0.82 and CEC 74meq/g dissolves in PetraSim, the volume fraction will decrease but the CEC will stay in 74meq/g. In real world though, if montmorillonite dissolves also the bentonite's capability to exchange cations will decrease.

In addition, one reason for the too high modelled pH can be explained by the fact that the crushed rock was considered as inert material. The diameter of one grain diameter was 1.5mm and hence the reactive area in the rock was quite large and thus the pH buffering capacity of the rock is supposedly notable.

Furthermore the absence of carbonates in this model may have effect on too high pH.

6.3 Mineral transformation

From **Figure 21** it can be seen that the mineral transformation of bentonite is quite small. The only notable change is that the gypsum dissolves totally. There is a small amount of secondary minerals brucite, tobermorite_14Å and hydrotalcite.

In other modelling studies **[Gaucher & Blanc, 2006]**, **[Savage et al., 2007]**, considering the interaction of high pH plume and bentonite, the results have indicated that within high pH plume and bentonite environment there will be formation of CSH-gels[13]. In this work how ever these gels did not occur.

One reason for this is that, as mentioned in **chapter 6.2**, in this model the montmorillonite does not dissolve and thus probably some phases, which would precipitate from montmorillonite's species, do not form here.

The porosity will stay constant during the simulation period. In PetraSim this evolving of porosity is possible to take into account but in this "learn to model"-work it was decided to keep it constant.

6.4 Other observations

There is also some other facts to keep in mind when comparing the modelling results to those from experiment. One of these is the diffusion coefficient. In this work it is assumed that all the diffusive ions have the same diffusion coefficient. In real world, however, all ions have characteristic diffusion coefficient. Choice, to use only one diffusion coefficient in this work, was made because the modeller can put only one diffusion coefficient to PetraSim.

[13] Calcium-silicate-hydrates

Thus the diffusion coefficient causes some of the uncertainty to the model but probably more uncertainty to the model is caused from the surface areas. As discussed in **section 3.3.4**, the reactive surface is quite difficult to measure and thus it causes uncertainty to modelling results. Furthermore, it should be noted that even if minerals surface area were well known at the beginning of the experiment, the surface area may change during the experiment. This evolving of the surface area is not greatly studied and PetraSim does not couple the dissolution (or precipitation) and the surface area evolving.

One notable point is also that in this work the concept of dispersion has not been taken into account. In this case it means that for example with better grid construction the evolution of pH would be a bit more realistic.

7 CONCLUSION

The main aim of the work was to learn how a couples hydro-chemical modelling procedure proceeds. For this, one experimental work **[Vuorinen et al., 2006]** was taken under modelling.

The modelling of this experiment needs understanding of different transport and chemical phenomena. The transport phenomena meant mainly the diffusion and advection, whereas the chemical reactions considered were cation exchange reactions on bentonite, mineral dissolution and precipitation on crushed rock material and bentonite.

The diffusion was assumed to happen in bentonite according to Fick's law and the advection, modelled with Darcy's law, was the transport phenomenon in crushed rock.

The modelling results indicated that the cation exchange phenomena were quite similar to the experimental results, whereas the pH results did not coincide with those of the experiment. Even though the modelling results and the experimental results, in terms of pH, were not in fact fully comparable, some kind of similar trend between model and experiment was expected, but not obtained.

In addition, the work considered some models of mineral alterations. The mineral alterations were quite small, mainly because of the short-duration of the experiment.

All in all this work gave a good overview of concepts needed in this demanding field and furthermore a better understanding on the chemical and transport phenomena and the theory behind them.

In the course of this work it became apparent that the terminology used in the bentonite field is inconsistent. This state of affair makes it difficult to see the point in articles and may even lead to misunderstandings.

In future the author is interested in understanding more about the surface complexes which seem to have a quite great role in this research area. In addition the author is keen on finding better ways to express these difficult and complicated phenomenon in a simpler way. Thus the author urges Finnish universities (and Posiva) to cooperation with each other.

REFERENCES

Anderson, G.M. 2005. Thermodynamics of Natural Systems. 2nd ed. Cambridge, United Kingdom: Cambridge University Press. 662.

Appelo, C.A.J. & Postma, D. 2005. Geochemistry, Groundwater and Pollution, Second Edition (PBK). 2nd ed. Amsterdam, Netherlands: Taylor & Francis. 649.

Barthelmy, D. , 2008, Mineralogy database, http://webmineral.com/.

Bethke, C.M. & Yeakel, S. 2009. GWB - Essentials guide. Urbana, Illinois, USA: Hydrogeology Program - University of Illinois. 116 p.

Blanc, P., Lassin, A. & Piantone, P. , 2008, THERMODDEM a database devoted to waste minerals, http://thermoddem.brgm.fr/.

Bradbury, M.H. & Baeyens, B. 2003. Porewater chemistry in compacted re-saturated MX-80 bentonite. *Journal of Contaminant Hydrology,* Vol. 61**, 1-4**, pp. 329-338.

Brantley, S.L., Kubicki, J.D. & White, A.F. 2007. Kinetics of Water-Rock Interaction. 1st ed. New York, USA: Springer Science+Business Media. 840.

Brunauer, S., Emmett, P.H. & Teller, E. 1938. Adsorption of Gases in Multimolecular Layers. *Journal of the American Chemical Society,* Vol. 60**, 2**, pp. 309-319.

Chapman, N.A. & McKinley, I.G. 1987. The Geological Disposal of Nuclear Waste. Great Britain: John Wiley & Sons. 292.

COMSOL AB 2008. Comsol Multiphysics version 3.5a, Earth Science Module, Model Library. www.comsol.com.

Elden, L., Wittmeyer-Koch, L. & Neilsen, H.B. 2004. Introduction To Numerical Computation: Analysis And MATLAB Illustrations. Sweden: Studentlitteratur AB. 375.

Gaucher, E.C. & Blanc, P. 2006. Cement/clay interactions – A review: Experiments, natural analogues, and modeling. *Waste Management,* Vol. 26**, 7**, pp. 776-788.

Harrington, J.F. & Horseman, S.T. 2003. Gas migration in KBS-3 buffer bentonite Sensitivity of test parameters to experimental boundary conditions. Stockholm, Sweden: SKB, Svensk Kärnbränslehantering AB. SKB-TR-03-02. 57 p.

Helgeson, H.C. & Kirkham, D. H. and Flowers G. C. 1981. Theoretical prediction of the thermodynamic behavior of aqueous electrolytes by high pressures and temperatures; IV, Calculation of activity coefficients, osmotic coefficients, and apparent molal and standard and relative partial molal properties to 600 degrees C and 5kb. *American Journal of Science,* Vol. 281**, 10**, pp. 1249-1516.

Huertas, F., Farias, J., Griffault, L., Leguey, S., Cuevas, C., Ramírez, S., Vigil de la Villa, R., Cobeña, J., Andrade, C., Alonso, M.C., Hidalgo, A., Parneix, J.C., Rassineux, F., Bouchet, A., Meunier, A., Decarraeau, A., Petit, S. & Vieillard, P. 2000. Effects of cement on clay barrier performance - Ecoclay project. Luxembourg: European Comission. EUR 19609. 141 p.

Jussila, P. 2007. Thermomechanics of swelling unsaturated porous media Compacted bentonite clay in spent fuel disposal. Doctor of Science in Technology ed. Yliopistopaino, Helsinki, Finland: STUK.

Langmuir, D. 1997. Aqueous Environmental Geochemistry. New Jersey, USA: Prentice Hall. 600.

Metcalfe, R. & Walker, C. 2004. Proceedings of the International Workshop on Bentonite-Cement Interaction in Repository Environments, 14-16 April 2004, Tokyo, Japan. Olkiluoto, Finland: Posiva Oy. Posiva-WR-2006-25. 192 p.

Montori, J., Soler, J.M. & Saaltink, M.W. 2008. Reactive transport modeling of the effect of hyperalkaline solutions along a fracture at the ONKALO site. Olkiluoto, Finland: Posiva Oy. Posiva-WR 2008-14. 105 p.

Ochs, M. & Talerico, C. 2004. SR-Can Data and uncertainty assessment Migration parameters for the bentonite buffer in the KBS-3 concept. Stockholm, Sweden: SKB, Svensk Kärnbränslehantering AB. SKB-TR-04-18. 165 p.

Odong, J. 2007. Evaluation of Empirical Formulae for Determination of Hydraulic Conductivity based on Grain-Size Analysis. *Journal of American Science,* Vol. 3**, 3**, pp. 54-60.

Olin, M. 1994. Hydrokemiallisten mallien käyttö spesiaatiotutkimuksessa. Espoo: VTT - Technical Research Centre of Finland. VTT Tiedotteita 1600. 1-49 p.

Palandri, J.L. & Kharaka, Y.K. 2004. A Compilation of Rate Parameters of Water-Mineral Interaction Kinetics for Application to Geochemical Modeling. , pp. 64.

Parkhurst, D.L. & Appelo, C.A.J. 1999. User's guide to PHREEQC (version 2) - A computer program for speciation, batch-reaction, one-dimensional transport, and inverse geochemical calculations. Denver, Colorado, U.S.A: U.S. Department of Interior. 312 p.

Pastina, B. & Hellä, P. 2008. Expected Evolution of a Spent Nuclear Fuel Repository at Olkiluoto (revised). Olkiluoto, Finland: Posiva Oy. Posiva-2006-05. 405 p.

Pruess, K., Oldenburg, C. & Moridis, G. 1999. TOUGH2 USER'S GUIDE, VERSION 2.0. 2.0th ed. Berkeley, California, USA: Lawrence Berkeley National Laboratory.

Reichl, L.E. 1980. A Modern Course in Statistical Physics. 1st ed. Great Britain: Ecward Arnold (publishers) LTD. 709.

Savage, D. & Benbow, S. 2007. Low pH Cements. Stockholm, Sweden: SKI, Swedish Nuclear Power Inspectorate. SKI-2007:32. 45 p.

Savage, D., Walker, C., Arthur, R., Rochelle, C., Oda, C. & Takase, H. 2007. Alteration of bentonite by hyperalkaline fluids: A review of the role of secondary minerals. *Physics and Chemistry of the Earth, Parts A/B/C*, Vol. 32**, 1-7**, pp. 287-297.

SKB, S.K.A. 2006. Long-term safety for KBS-3 repositories at Forsmark and Laxemar - a first evaluation. Main report of the SR-Can project. Stockholm, Sweden: SKB, Svensk Kärnbränslehantering AB. SKB-TR-06-09. 620 p.

STUK , 2008, Säteilyturvakeskus, Radiation and Nuclear Authority, http://www.stuk.fi/.

Stumm, W. & Morgan, J.J. 1996. Aquatic Chemistry. 3rd ed. Wiley-Interscience. 22.

The COMSOL Group , 2009, COMSOL multiphysics, http://www.comsol.com/.

The Engineering ToolBox , 2005, Water - Dynamic and Kinematic Viscosity Viscosity of water at temperatures between 0 - 100°C (32 - 212°F) - in Imperial and SI Units, http://www.engineeringtoolbox.com/water-dynamic-kinematic-viscosity-d_596.html.

Thunderhead engineering 2005. PetraSim User Manual.

Tournassat, C., Gailhanou, H., Crouzet, C., Braibant, G., Gautier, A., Lassin, A., Blanc, P. & Gaucher, E.C. 2007. Two cation exchange models for direct and inverse modelling of solution major cation composition in equilibrium with illite surfaces. *Geochimica et Cosmochimica Acta*, Vol. 71**, 5**, pp. 1098-1114.

Vuorinen, U., Lehikoinen, J., Luukkonen, A. & Ervanne, H. 2006. Effects of Salinity and High pH on Crushed Rock and Bentonite - Experimental Work and Modelling. Olkiluoto, Finland: Posiva Oy. Posiva-2006-01. 116 p.

Wolery, T.W. & Jarek, R.L. 2003. SOFTWARE USER'S MANUAL EQ3/6, Version 8.0. Las Vegas, Nevada: Sandia National Laboratories. 118 p.

Xu, T., Sonnenthal, E., Spycher, N. & Pruess, K. 2004. TOUGHREACT User's Guide: A Simulation Program for Nonisothermal Multiphase Reactive Geochemical Transport in Variably Saturated Geologic Media. Berkeley, California, USA: Lawrence Berkeley National Laboratory.

Zhu, C. & Anderson, G. 2002. Environmental Applications of Geochemical Modeling. 1st ed. Cambridge, United Kingdom: Cambridge University Press. 298.

APPENDIX A

Table A - 1Parameters for different materials (bentonite and crushed rock) used in the modeling.

	bentonite	*crushed rock*	H_20	H^+	Na^+	Ca^{2+}	K^+	Mg^{2+}	Cl^-	Al^{3+}	H_4SiO_4, SO_4^{2-}
density	2.75	2.65									
porosity	0.438	0.285									
permeability [m^2]	1.0e-21	5.0e-11									
tortuosity	0.13	0.53									
initial water	x	x	1.0	1.0E-7	10.0E-06	9.7E-12	39.0E-09	5.4E-12	1.000E-5	1.0E-8	10.0E-9
inflow water		x	1.0	0.316228E-12	0.428	0.018	1.0E-8	1.0E-8	0.462	1.0E-20	10.0E-9
mineral composition	x (see table 4)	not considered because crushed rock were assumed to be inert									
kinetic parameters for minerals	x (see table 2)										

APPENDIX B

The database information of used basis and secondary species. The database is from **[Blanc et al. , 2008]** with the exception of CSH phases, from **[Montori et al. , 2008]** and K-feldspar from TOUGHREACT's original database ThermXu4.dat

```
'H2O'                    0.00  0.00    18.015
'H+'                    3.08  1.00     1.008
'Al+++'                  3.33  3.00    26.982
'Ca++'                   2.87  2.00    40.078

'Cl-'                   1.81 -1.00    35.453
'H4SiO4(aq)'                0.00  0.00    96.115
'K+'                    2.27  1.00    39.102
'Mg++'                   2.54  2.00    24.312
'Na+'                   1.91  1.00    22.990

'Albite'                262.225   100.430    5  -4.0000 'H+'  -4.0000 'H2O'  1.0000 'Al+++'  1.0000 'Na+'  3.0000 'H4SiO4(aq)'
'Albite'                   4.0542    2.7406    1.2039   -0.2300   -1.7026   -2.9656   -4.1262   -5.2627
'Albite'                0.91148580E+02   -0.58378623E+03   -0.95590038E-01    0.34064563E+05   -0.16492377E+07

'Brucite'                58.327    24.630    3  -2.0000 'H+'  1.0000 'Mg++'  2.0000 'H2O'
'Brucite'                  18.9424   17.1020   15.0199   13.1564   11.3532    9.9359    8.7631    7.7339
'Brucite'               0.56990120E+02   -0.36338229E+03   -0.54069199E-01    0.24724483E+05   -0.98022474E+06

'Cristobalite'             60.085    27.440    2  -2.0000 'H2O'  1.0000 'H4SiO4(aq)'
'Cristobalite'               -3.3794   -3.1067   -2.8026   -2.5314   -2.2661   -2.0550   -1.8792   -1.7264
'Cristobalite'            -0.15513660E+01    0.82713723E+01    0.25601073E-02   -0.85838890E+03   -0.37633216E+05
```

```
'Ettringite'          1255.100   710.320    5 -12.0000 'H+'  2.0000 'Al+++'  6.0000 'Ca++'  38.0000 'H2O'  3.0000 'SO4--'
'Ettringite'            62.9688   57.0086   49.8929   43.1581   36.0835   29.7782   23.5695   16.6430
'Ettringite'          0.11202457E+04  -0.71062012E+04  -0.11015987E+01   0.40532116E+06  -0.22265400E+08

'Friedel_Salt'         561.331   276.240    5 -12.0000 'H+'  2.0000 'Al+++'  4.0000 'Ca++'  2.0000 'Cl-'  16.0000 'H2O'
'Friedel_Salt'          82.7147   74.9463   65.9830   57.7624   49.5225   42.7031   36.6451   30.7628
'Friedel_Salt'        0.55776214E+03  -0.35365450E+04  -0.55121311E+00   0.21383533E+06  -0.10601225E+08

'Gibbsite'             78.004    31.956    3  -3.0000 'H+'  1.0000 'Al+++'  3.0000 'H2O'
'Gibbsite'              9.3859    7.7380    5.8512    4.1324    2.4165    0.9988   -0.2533   -1.4307
'Gibbsite'            0.80765125E+02  -0.51642358E+03  -0.83829787E-01   0.31068372E+05  -0.13524838E+07

'Gypsum'               172.170    74.690    3   1.0000 'Ca++'  2.0000 'H2O'  1.0000 'SO4--'
'Gypsum'                -4.6623   -4.6047   -4.7141   -4.9860   -5.4804   -6.1370   -7.0009   -8.2157
'Gypsum'              0.27567396E+03  -0.17539906E+04  -0.27403825E+00   0.97390931E+05  -0.58872949E+07

'Hydrotalcite'         443.360   227.360    4 -14.0000 'H+'  2.0000 'Al+++'  4.0000 'Mg++'  17.0000 'H2O'
'Hydrotalcite'          82.3710   73.7573   63.9365   55.0798   46.4128   39.4733   33.5709   28.2080
'Hydrotalcite'        0.37796264E+03  -0.24100672E+04  -0.36670128E+00   0.15406974E+06  -0.68509419E+07

'KatoiteSi1'           402.340   130.700    5 -12.0000 'H+'  2.0000 'Al+++'  3.0000 'Ca++'  8.0000 'H2O'  1.0000 'H4SiO4(aq)'
'KatoiteSi1'            79.9243   71.1681   61.1468   52.0360   43.0428   35.8027   29.6573   24.1309
'KatoiteSi1'          0.29820591E+03  -0.19047432E+04  -0.29675178E+00   0.12680123E+06  -0.53296918E+07

'K-feldspar'           278.330   108.870    5   1.0000 'K+'  3.0000 'H4SiO4(aq)'  -4.0000 'H+' -4.0000 'H2O'  1.0000 'Al+++'
'K-feldspar'            0.9340   -0.0270   -1.0480   -1.9440   -2.8730   -3.7450   -4.5740   -5.4140
'K-feldspar'          -0.13247959E+02   0.10268505E+03  -0.14088105E-01  -0.11529375E+05   0.13899054E+07
```

```
'Monosulfoaluminate'          622.517   311.260    5 -12.0000 'H+'  2.0000 'Al+++'  4.0000 'Ca++'  18.0000 'H2O'  1.0000 'SO4--'
'Monosulfoaluminate'            81.0749   72.7483   63.0771   54.1258   45.0403   37.4088   30.5460   23.8510
'Monosulfoaluminate'          0.58422687E+03  -0.37030755E+04  -0.59094304E+00   0.22271934E+06  -0.10992828E+08

'Muscovite'                   398.313   140.710    4 -10.0000 'H+'  3.0000 'Al+++'  1.0000 'K+'  3.0000 'H4SiO4(aq)'
'Muscovite'                     15.4932   11.3367    6.5123    2.0514   -2.4760   -6.2883   -9.7197  -13.0052
'Muscovite'                   0.23908312E+03  -0.15348609E+04  -0.24944607E+00   0.91333286E+05  -0.42633226E+07

'Portlandite'                  74.093    33.056    3  -2.0000 'H+'  1.0000 'Ca++'  2.0000 'H2O'
'Portlandite'                    24.9055   22.8120   20.4285   18.2713   16.1578   14.4806   13.0897   11.8758
'Portlandite'                 0.46720651E+02  -0.29446949E+03  -0.45897105E-01   0.21973574E+05  -0.79362435E+06

'Quartz'                      60.085    22.690    2  -2.0000 'H2O'  1.0000 'H4SiO4(aq)'
'Quartz'                        -4.0786   -3.7398   -3.3491   -2.9907   -2.6346   -2.3507   -2.1170   -1.9184
'Quartz'                     -0.24026733E+01   0.15077782E+02   0.25455833E-02  -0.19142005E+04   0.47386294E+05

'Straetlingite'               409.316   215.630    5 -10.0000 'H+'  2.0000 'Al+++'  2.0000 'Ca++'  10.5000 'H2O'  1.0000 'H4SiO4(aq)'
'Straetlingite'                 56.2472   49.6707   42.2112   35.5097   28.9841   23.7974   19.4319   15.5189
'Straetlingite'               0.24580307E+03  -0.15740436E+04  -0.23844316E+00   0.10207688E+06  -0.42707561E+07

'Tobermorite'                 739.980   286.190    4 -10.0000 'H+'  -1.5000 'H2O'  5.0000 'Ca++'  6.0000 'H4SiO4(aq)'
'Tobermorite'                   71.5844   65.5785   58.7825   52.6929   46.8058   42.1856   38.3638   34.9775
'Tobermorite'                 0.21929645E+03  -0.13911962E+04  -0.20489990E+00   0.93412789E+05  -0.39911153E+07

'Tobermorite_14A'             830.057   351.300    4 -10.0000 'H+'  5.0000 'Ca++'  3.5000 'H2O'  6.0000 'H4SiO4(aq)'
'Tobermorite_14A'               67.9411   62.9436   57.3971   52.5544   48.0200   44.5806   41.8103   39.3765
'Tobermorite_14A'             0.22098179E+03  -0.13964905E+04  -0.19780884E+00   0.90278438E+05  -0.38617542E+07
```

```
'C3AH6'                 378.285   149.520    4 -12.0000 'H+'  2.0000 'Al+++'  3.0000 'Ca++'  12.0000 'H2O'
'C3AH6'                   89.7191   80.3322   69.6179   59.8968   50.3092   42.5886   36.0295   30.1283
'C3AH6'                 0.30821848E+03   -0.19605304E+04   -0.31052397E+00    0.13019000E+06   -0.52724619E+07

'CSH_0.0'               60.08    27.31       2    1.0000 'H4SiO4(aq)' -2.0000 'H2O'
'CSH_0.0'                  0.0 -1.2000 0.0 0.0 0.0 0.0 0.0 0.0
'CSH_0.0'               -14.814    95.578    0.012713    -6470.1    352730

'CSH_0.4'               125.008   56.82      4   0.5600 'Ca++' -1.6600 'H2O' -1.1200 'H+' 1.3900 'H4SiO4(aq)'
'CSH_0.4'                  0.0 6.4767 0.0 0.0 0.0 0.0 0.0 0.0
'CSH_0.4'               1.8244    -11.599   -0.000066655    4818.2     -2105.9

'CSH_0.8'               132.690    59.290    4   1.8200 'Ca++' -0.9000 'H2O' -3.6400 'H+' 2.2700 'H4SiO4(aq)'
'CSH_0.8'                  0.0 24.6311 0.0 0.0 0.0 0.0 0.0 0.0
'CSH_0.8'               5.747    -34.874    -0.000033052    17550    -758.26

'CSH_1.2'               164.489    71.950    4   1.2000 'Ca++'  0.4000 'H2O' -2.4000 'H+' 1.0000 'H4SiO4(aq)'
'CSH_1.2'                  0.00000 18.8013 0.00000 0.00000 0.00000 0.00000 0.00000 0.00000
'CSH_1.2'               4.0692    -27.419    -0.00030931    14229    -9412.8

'CSH_1.667'                196.288    84.680    4   1.6670 'Ca++'  1.3340 'H2O' -3.3340 'H+' 1.0000 'H4SiO4(aq)'
'CSH_1.667'                  0.00000  29.1328 0.00000 0.00000 0.00000 0.00000 0.00000 0.00000
'CSH_1.667'                4.8947    -34.103    0.00015461    21827    3574.4
```

APPENDIX C

Table C - 1. The results of chemical components at selected times. The concentrations are in units: mol/kg H_2O.

TIME (s)		Ca++	K+	Mg++	Na+
0	A1	0.108935	3.22E-02	5.25E-02	2.082886
0	A2	0.108935	3.22E-02	5.25E-02	2.082886
0		0	0	0	0
0		0	0	0	0
0	B1	0.108935	3.22E-02	5.25E-02	2.082886
0	B2	0.108935	3.22E-02	5.25E-02	2.082886
0	C1	0.108935	3.22E-02	5.25E-02	2.082886
0	C2	0.108935	3.22E-02	5.25E-02	2.082886
0	D1	0.108935	3.22E-02	5.25E-02	2.082886
0	D2	0.108935	3.22E-02	5.25E-02	2.082886
0		0	0	0	0
0		0	0	0	0
0	E1	0.108935	3.22E-02	5.25E-02	2.082886
0	E2	0.108935	3.22E-02	5.25E-02	2.082886
0	F1	0.108935	3.22E-02	5.25E-02	2.082886
0	F2	0.108935	3.22E-02	5.25E-02	2.082886
0		0	0	0	0
0		0	0	0	0
0		0	0	0	0
0		0	0	0	0
31100000	A1	0.120135	1.08E-02	1.38E-06	2.187786
31100000	A2	0.119782	1.91E-02	1.39E-06	2.176391
31100000		0	0	0	0
31100000		0	0	0	0
31100000	B1	0.120184	1.29E-02	1.38E-06	2.186809
31100000	B2	0.119782	2.07E-02	1.39E-06	2.174195
31100000	C1	0.120235	1.50E-02	1.39E-06	2.185556
31100000	C2	0.119811	2.24E-02	1.39E-06	2.172083
31100000	D1	0.120252	1.69E-02	1.39E-06	2.183884
31100000	D2	0.119827	2.38E-02	1.39E-06	2.170343
31100000		0	0	0	0
31100000		0	0	0	0
31100000	E1	0.120242	1.86E-02	1.39E-06	2.18221
31100000	E2	0.119812	2.51E-02	1.40E-06	2.168944
31100000	F1	0.120178	2.02E-02	1.39E-06	2.180345
31100000	F2	0.119763	2.61E-02	1.40E-06	2.167878
31100000		0	0	0	0
31100000		0	0	0	0
31100000		0	0	0	0
31100000		0	0	0	0
48380000	A1	0.119634	8.29E-03	1.38E-06	2.191669
48380000	A2	0.118877	1.46E-02	1.39E-06	2.183006
48380000		0	0	0	0
48380000		0	0	0	0

48380000	B1	0.119569	1.01E-02	1.38E-06	2.191307
48380000	B2	0.118778	1.61E-02	1.39E-06	2.181153
48380000	C1	0.119509	1.19E-02	1.39E-06	2.190559
48380000	C2	0.118698	1.78E-02	1.39E-06	2.179289
48380000	D1	0.119432	1.36E-02	1.39E-06	2.189274
48380000	D2	0.118636	1.93E-02	1.39E-06	2.177632
48380000		0	0	0	0
48380000		0	0	0	0
48380000	E1	0.119351	1.52E-02	1.39E-06	2.18789
48380000	E2	0.118576	2.07E-02	1.40E-06	2.17619
48380000	F1	0.11923	1.66E-02	1.39E-06	2.18625
48380000	F2	0.118502	2.18E-02	1.40E-06	2.175036
48380000		0	0	0	0
48380000		0	0	0	0
48380000		0	0	0	0
48380000		0	0	0	0

APPENDIX D

Table D - 1. The modelling results at selected times.

TIME (s)		P (bar)	Sl	T (C)	pH	Porosity	Perm (m^2)	Albite	Cristobalite	Gypsum	Muscovite	Quartz	Brucite	Tobermorite_14A	Hydrotalcite
0	A1	1.013	1	25	7	0.438	1.00E-21	4.13E-02	2.04E-02	6.73E-04	5.49E-03	2.95E-02	0	0	0
0	A2	1.013	1	25	7	0.438	1.00E-21	4.13E-02	2.04E-02	6.73E-04	5.49E-03	2.95E-02	0	0	0
0		1.013	1	25	7	0.27	5.00E-11	0	0	0	0	0	0	0	0
0		1.013	1	25	7	0.27	5.00E-11	0	0	0	0	0	0	0	0
0	B1	1.013	1	25	7	0.438	1.00E-21	4.13E-02	2.04E-02	6.73E-04	5.49E-03	2.95E-02	0	0	0
0	B2	1.013	1	25	7	0.438	1.00E-21	4.13E-02	2.04E-02	6.73E-04	5.49E-03	2.95E-02	0	0	0
0	C1	1.013	1	25	7	0.438	1.00E-21	4.13E-02	2.04E-02	6.73E-04	5.49E-03	2.95E-02	0	0	0
0	C2	1.013	1	25	7	0.438	1.00E-21	4.13E-02	2.04E-02	6.73E-04	5.49E-03	2.95E-02	0	0	0
0	D1	1.013	1	25	7	0.438	1.00E-21	4.13E-02	2.04E-02	6.73E-04	5.49E-03	2.95E-02	0	0	0
0	D2	1.013	1	25	7	0.438	1.00E-21	4.13E-02	2.04E-02	6.73E-04	5.49E-03	2.95E-02	0	0	0
0		1.013	1	25	7	0.27	5.00E-11	0	0	0	0	0	0	0	0
0		1.013	1	25	7	0.27	5.00E-11	0	0	0	0	0	0	0	0
0	E1	1.013	1	25	7	0.438	1.00E-21	4.13E-02	2.04E-02	6.73E-04	5.49E-03	2.95E-02	0	0	0
0	E2	1.013	1	25	7	0.438	1.00E-21	4.13E-02	2.04E-02	6.73E-04	5.49E-03	2.95E-02	0	0	0
0	F1	1.013	1	25	7	0.438	1.00E-21	4.13E-02	2.04E-02	6.73E-04	5.49E-03	2.95E-02	0	0	0
0	F2	1.013	1	25	7	0.438	1.00E-21	4.13E-02	2.04E-02	6.73E-04	5.49E-03	2.95E-02	0	0	0
0		1.013	1	25	7	0.27	5.00E-11	0	0	0	0	0	0	0	0
0		1.013	1	25	7	0.27	5.00E-11	0	0	0	0	0	0	0	0
0		1.013	1	25	7	0.27	5.00E-11	0	0	0	0	0	0	0	0
0		1.013	1	25	7	0.27	5.00E-11	0	0	0	0	0	0	0	0
31100000	A1	1.013	1	25	12.21866	0.438	1.00E-20	4.13E-02	2.04E-02	0	5.48E-03	2.95E-02	6.74E-04	8.20E-05	4.79E-05
31100000	A2	1.013	1	25	12.21584	0.438	1.00E-20	4.13E-02	2.04E-02	0	5.48E-03	2.95E-02	3.09E-04	6.19E-05	4.03E-05
31100000		1.013	1	25	12.22166	0.27	5.00E-11	0	0	0	0	0	0	0	0
31100000		1.013	1	25	12.22084	0.27	5.00E-11	0	0	0	0	0	0	0	0
31100000	B1	1.013	1	25	12.21787	0.438	1.00E-20	4.13E-02	2.04E-02	0	5.48E-03	2.95E-02	8.11E-04	7.59E-05	4.56E-05
31100000	B2	1.013	1	25	12.21519	0.438	1.00E-20	4.13E-02	2.04E-02	0	5.48E-03	2.95E-02	2.55E-04	5.90E-05	3.87E-05

31100000	C1	1.013	1	25	12.21706	0.438	1.00E-20	4.13E-02	2.04E-02	0	5.48E-03	2.95E-02	9.10E-04	7.00E-05	4.31E-05
31100000	C2	1.013	1	25	12.21439	0.438	1.00E-20	4.13E-02	2.04E-02	0	5.48E-03	2.95E-02	2.21E-04	5.54E-05	3.67E-05
31100000	D1	1.013	1	25	12.21627	0.438	1.00E-20	4.13E-02	2.04E-02	0	5.48E-03	2.95E-02	9.41E-04	6.46E-05	4.07E-05
31100000	D2	1.013	1	25	12.21359	0.438	1.00E-20	4.13E-02	2.04E-02	0	5.48E-03	2.95E-02	2.00E-04	5.16E-05	3.47E-05
31100000		1.013	1	25	12.22007	0.27	5.00E-11	0	0	0	0	0	0	0	0
31100000		1.013	1	25	12.21917	0.27	5.00E-11	0	0	0	0	0	0	0	0
31100000	E1	1.013	1	25	12.21552	0.438	1.00E-20	4.13E-02	2.04E-02	0	5.48E-03	2.95E-02	9.51E-04	5.98E-05	3.85E-05
31100000	E2	1.013	1	25	12.21285	0.438	1.00E-20	4.13E-02	2.04E-02	0	5.48E-03	2.95E-02	1.84E-04	4.80E-05	3.28E-05
31100000	F1	1.013	1	25	12.21494	0.438	1.00E-20	4.13E-02	2.04E-02	0	5.48E-03	2.95E-02	9.08E-04	5.60E-05	3.65E-05
31100000	F2	1.013	1	25	12.21232	0.438	1.00E-20	4.13E-02	2.04E-02	0	5.48E-03	2.95E-02	1.70E-04	4.51E-05	3.13E-05
31100000		1.013	1	25	12.21869	0.27	5.00E-11	0	0	0	0	0	0	0	0
31100000		1.013	1	25	12.2178	0.27	5.00E-11	0	0	0	0	0	0	0	0
31100000		1.013	1	25	12.21929	0.27	5.00E-11	0	0	0	0	0	0	0	0
31100000		1.013	1	25	12.21838	0.27	5.00E-11	0	0	0	0	0	0	0	0
48380000	A1	1.013	1	25	12.21889	0.438	1.00E-20	4.13E-02	2.04E-02	0	5.48E-03	2.95E-02	6.60E-04	1.34E-04	7.95E-05
48380000	A2	1.013	1	25	12.21625	0.438	1.00E-20	4.13E-02	2.04E-02	0	5.48E-03	2.95E-02	2.95E-04	1.14E-04	7.19E-05
48380000		1.013	1	25	12.22173	0.27	5.00E-11	0	0	0	0	0	0	0	0
48380000		1.013	1	25	12.22096	0.27	5.00E-11	0	0	0	0	0	0	0	0
48380000	B1	1.013	1	25	12.21816	0.438	1.00E-20	4.13E-02	2.04E-02	0	5.48E-03	2.95E-02	7.98E-04	1.28E-04	7.72E-05
48380000	B2	1.013	1	25	12.21568	0.438	1.00E-20	4.13E-02	2.04E-02	0	5.48E-03	2.95E-02	2.41E-04	1.11E-04	7.02E-05
48380000	C1	1.013	1	25	12.21744	0.438	1.00E-20	4.13E-02	2.04E-02	0	5.48E-03	2.95E-02	8.96E-04	1.22E-04	7.47E-05
48380000	C2	1.013	1	25	12.21498	0.438	1.00E-20	4.13E-02	2.04E-02	0	5.48E-03	2.95E-02	2.08E-04	1.07E-04	6.82E-05
48380000	D1	1.013	1	25	12.21674	0.438	1.00E-20	4.13E-02	2.04E-02	0	5.48E-03	2.95E-02	9.27E-04	1.16E-04	7.23E-05
48380000	D2	1.013	1	25	12.2143	0.438	1.00E-20	4.13E-02	2.04E-02	0	5.48E-03	2.95E-02	1.86E-04	1.03E-04	6.62E-05
48380000		1.013	1	25	12.22026	0.27	5.00E-11	0	0	0	0	0	0	0	0
48380000		1.013	1	25	12.21942	0.27	5.00E-11	0	0	0	0	0	0	0	0
48380000	E1	1.013	1	25	12.2161	0.438	1.00E-20	4.13E-02	2.04E-02	0	5.48E-03	2.95E-02	9.37E-04	1.12E-04	7.00E-05
48380000	E2	1.013	1	25	12.21368	0.438	1.00E-20	4.13E-02	2.04E-02	0	5.48E-03	2.95E-02	1.71E-04	9.98E-05	6.43E-05
48380000	F1	1.013	1	25	12.21561	0.438	1.00E-20	4.13E-02	2.04E-02	0	5.48E-03	2.95E-02	8.94E-04	1.08E-04	6.80E-05
48380000	F2	1.013	1	25	12.21326	0.438	1.00E-20	4.13E-02	2.04E-02	0	5.48E-03	2.95E-02	1.57E-04	9.68E-05	6.27E-05
48380000		1.013	1	25	12.21903	0.27	5.00E-11	0	0	0	0	0	0	0	0

48380000	1.013	1	25	12.21822	0.27	5.00E-11	0	0	0	0	0	0	0	0
48380000	1.013	1	25	12.21968	0.27	5.00E-11	0	0	0	0	0	0	0	0
48380000	1.013	1	25	12.21884	0.27	5.00E-11	0	0	0	0	0	0	0	0

APPENDIX E

The used program does not print out the amount of cations in eq/g **bentonite** but as mol/g **water** thus some post-calculations need to be done. It also needs to take into account that the PetraSim (and TOUGHREACT) has the bug mentioned in **chapter 4.8.2**. Thus also the **equation (4-19)** needs to be used before the results can be shown like in **Figure 18 and 19**

Thus the post-calculation consists of two steps, first the eq/g **water** need to be changed to eq/g **bentonite**. The equation for this unit change (from eq/g of water to eq/g of bentonite) is derived in the following way.

The total volume V of the body consists of material and the pores thus the volume of the pores V_w is

$$V_w = \phi V \tag{4-29}$$

and volume of solid is

$$V_s = (1-\phi)V \tag{4-30}$$

Furhermore the mass for water in pores is

$$m_w = \rho_w \phi V \tag{4-31}$$

and mass for solid is

$$m_s = \rho_s (1-\phi)V \tag{4-32}$$

Still the concentration of element in water c_w is

$$c_w = \frac{M}{m_w} \tag{4-33}$$

and for solid c_s

$$c_s = \frac{M}{m_s} \tag{4-34}$$

where M is the amount of species in moles, m_w is mass of water in grams and m_s is mass of solid in grams.

Furhermore adding **equations (4-34)**, **(4-33)** and still equations **(4-32)** and **(4-31)** we get:

$$\begin{aligned} c_s &= \frac{m_w}{m_s} c_w \\ &= \frac{\rho_s (1-\phi) V}{\rho_w \phi V} c_w = \frac{\rho_s (1-\phi)}{\rho_w \phi} c_w \end{aligned} \tag{4-35}$$

Thus the results from PetraSim (and TOUGHREACT) need to be multiplied by **equation (4-35)**.

And secondly the **equation (4-19)** need to be used 'backwards' to get right answers. Thus

$$CEC_{\text{input}} = CEC_{\text{experiment}} \frac{\rho_{\text{material}}}{2.65 \, \text{g}/\text{cm}^3} \tag{4-36}$$

which yields

$$\Rightarrow c_{\text{experiment}} = z \cdot c_{\text{PetraSim result}} \frac{2.65 \, \text{g}/\text{cm}^3}{\rho_{\text{material}}} \tag{4-37}$$

where z is charge of the ion (2 for Ca^{2+}), c_{PetraSim} is the result from PetraSim and ρ_{material} is the density of the material.

So as a conclusion, the results from PetraSim needs to be calculated like in **equation (4-38)** to get the results in **Figure 18** and **Figure 19**.

$$c_{\text{final result}} = z \cdot \frac{2.65 \, \text{g}/\text{cm}^3}{\rho_{\text{material}}} \cdot \frac{\rho_s (1-\phi)}{\rho_w \phi} c_{\text{PetraSim result}} \tag{4-38}$$